

Lawrence Berkeley National Laboratory

Recent Work

Title

Secondary building units as the turning point in the development of the reticular chemistry of MOFs.

Permalink

<https://escholarship.org/uc/item/8m17s9f1>

Journal

Science advances, 4(10)

ISSN

2375-2548

Authors

Kalmutzki, Markus J

Hanikel, Nikita

Yaghi, Omar M

Publication Date

2018-10-01

DOI

10.1126/sciadv.aat9180

Peer reviewed

CHEMISTRY

Secondary building units as the turning point in the development of the reticular chemistry of MOFs

Markus J. Kalmutzki^{1,2}, Nikita Hanikel^{1,2}, Omar M. Yaghi^{1,2,3,*†}

The secondary building unit (SBU) approach was a turning point in the discovery of permanently porous metal-organic frameworks (MOFs) and in launching the field of reticular chemistry. In contrast to the single-metal nodes known in coordination networks, the polynuclear nature of SBUs allows these structures to serve as rigid, directional, and stable building units in the design of robust crystalline materials with predetermined structures and properties. This concept has also enabled the development of MOFs with ultra-high porosity and structural complexity. The architectural, mechanical, and chemical stability of MOFs imparted by their SBUs also gives rise to unique framework chemistry. All of this chemistry—including ligand, linker, metal exchange, and metallation reactions, as well as precisely controlled formation of ordered vacancies—is carried out with full retention of the MOF structure, crystallinity, and porosity. The unique chemical nature of SBUs makes MOFs useful in many applications including gas and vapor adsorption, separation processes, and SBU-mediated catalysis. In essence, the SBU approach realizes a long-standing dream of scientists by bringing molecular chemistry (both organic and inorganic) to extended solid-state structures. This contribution highlights the importance of the SBUs in the development of MOFs and points to the tremendous potential still to be harnessed.

INTRODUCTION

Progress in solving societal challenges relies heavily on the discovery of new materials. In the last century, the approach to making solid-state structures has been largely serendipitous. Although this approach has led to important discoveries and will continue to do so, there is an urgent need for control of materials on the molecular level to make “materials on demand” (1, 2). A strategy for developing these materials is being realized in reticular chemistry (from Latin “reticulum” meaning “having the form of a net” or “netlike”), the study of linking discrete building units (molecules and clusters) by strong bonds to make large and extended crystalline structures. Undoubtedly, the most prominent class of materials within the realm of reticular chemistry is metal-organic frameworks (MOFs)—crystalline extended structures constructed by stitching together inorganic polynuclear clusters [termed secondary building units (SBUs)] and organic linkers by strong bonds (3). The term SBU was originally used as an intellectual tool in the description of zeolites, where primary building units (that is, TO_4 tetrahedra) form larger periodically recurring structural arrangements (that is, SBUs) (4). The past two decades have seen an explosive growth of the MOF field. The Cambridge Crystallographic Data Centre documents 84,185 MOF structures as of 7 June 2018 (5), and thousands of papers on the synthesis, structure, and applications of MOFs are published every year. Among the many advances made in MOF chemistry, introduction of the SBU approach not only gave rise to the field of MOF chemistry itself: It also has been the most significant contributor to this rapid development. Today, the vast majority of MOF syntheses, investigations, and applications are derived from the SBU approach.

FROM SINGLE-METAL NODES TO SBUS

To appreciate the impact of the SBU approach on the development of MOFs, it is instructive to briefly consider the history of extended

metal-organic compounds. Coordination networks in which single-metal nodes such as Cu^+ are joined together by neutral organic donor linkers based on nitriles [for example, adiponitrile = $\text{NC}(\text{CH}_2)_4\text{CN}$] have been known since 1959 (6). Pyridine-based linkers (for example, 4,4'-bipyridine) have also been used to construct these networks (7). The late 1980s and 1990s witnessed a large number of studies in which the metal ions and neutral donor linkers were varied to produce coordination networks. These compounds adopted a handful of structure types whose number is limited by the coordination geometries that can be realized using single-metal nodes (7–10). Although these coordination networks were described as porous, proof of permanent porosity was absent. Their structures were frail and lacked architectural stability, due to the weak nondirectional bonds linking their constituents and flexibility around the single-metal nodes. Thus, coordination networks were in fact nonporous, and their structures collapsed upon removal of guest molecules. In 1998, the reticulation of Zn^{2+} ions with a charged organic linker (BDC^{2-} = 1,4-benzene dicarboxylate) resulted in the formation of a MOF termed MOF-2 [$\text{Zn}_2(\text{BDC})_2(\text{H}_2\text{O})_2$], where dinuclear zinc paddle wheel clusters [$\text{Zn}_2(-\text{COO})_4(\text{H}_2\text{O})_2$] served as the nodes to form stacked two-dimensional (2D) porous layers (11). The polynuclear cluster nodes (termed SBUs) ensured (i) thermodynamic stability, because the framework is entirely composed of strong bonds ($\text{Zn}-\text{O}$, $\text{C}-\text{O}$, and $\text{C}-\text{C}$) (12), and (ii) mechanical and architectural stability originating from strong directional bonds, locking down the position of the metal centers in the SBUs. These attributes contrast with those of single-metal nodes, which are unsteady and nondirectional and make weak bonds to neutral organic donor linkers.

The original evidence that dinuclear paddle wheel SBUs were key to creating architecturally stable and permanently porous MOFs was obtained by nitrogen adsorption isotherm measurements at 77 K and low pressure performed on MOF-2. The surface area and pore volume ($S_{\text{Lang.}} = 310 \text{ m}^2 \text{ g}^{-1}$, $V_p = 0.10 \text{ cm}^3 \text{ cm}^{-3}$) determined for this MOF allowed, for the first time, comparison to more established porous crystals such as zeolites. It should be mentioned here that the uptake of gases at room temperature and high pressure as observed for some coordination networks (13) does not in itself provide real evidence of permanent porosity, which can be determined

Copyright © 2018
The Authors, some
rights reserved;
exclusive licensee
American Association
for the Advancement
of Science. No claim to
original U.S. Government
Works. Distributed
under a Creative
Commons Attribution
NonCommercial
License 4.0 (CC BY-NC).

¹Department of Chemistry, Kavli Energy NanoScience Institute, and Berkeley Global Science Institute, University of California, Berkeley, Berkeley, CA 94720, USA. ²Materials Sciences Division, Lawrence Berkeley National Laboratory, Berkeley, CA 94720, USA. ³King Abdulaziz City for Science and Technology, Riyadh 11442, Saudi Arabia. *On the occasion of the BBVA Frontiers of Knowledge Award in the Basic Sciences 2018. †Corresponding author. Email: yaghi@berkeley.edu

only by gas adsorption isotherms at the boiling point of the adsorbent and low pressure – the gold standard for determining porosity, as with porosity measurements for MOF-2.

Other studies have followed the same approach as that used in the synthesis of MOF-2, but using tetranuclear basic zinc acetate cluster $[Zn_4O(-COO)_6]$ as the SBU. The reticulation of these SBUs using BDC linkers yielded MOF-5 $[Zn_4O(BDC)_3]$, which combined exceptional architectural stability, porosity, and ultra-high surface area (14). The report of MOF-5 and other 3D MOFs using the SBU approach developed in the MOF-2 study {for example, HKUST-1 $[Cu_3(BTC)_2(H_2O)_3]$, where BTC = benzene-1,3,5-tricarboxylate} (15) lent credence to the applicability of SBUs to the synthesis of 3D permanently porous frameworks with high surface areas. The porosity of MOFs is useful for introducing molecules into their pores and for carrying out chemical transformations within the pores and onto the frameworks in ways not otherwise possible. These transformations include ligand, linker, and metal ion exchange reactions, substitution reactions, the functionalization of the organic backbone by post-synthetic methods, and the catalytic transformation of guest molecules.

The exceptional architectural stability of MOF-5 can be explained by considering the envelope representation of its crystal structure. The envelope of the $Zn_4O(-COO)_6$ SBU is of truncated tetrahedral shape, and that of the BDC linker is of rectangular planar shape. In the **pcu** net of MOF-5, the envelopes of the linker molecules located at opposing sides of the 6-c SBUs are rotated against each other by 90°, thereby eliminating all stress at the center of the nodes. This arrangement, in combination with the rigid nature of the SBU, leads to outstanding mechanical and architectural stability (3).

The reports of MOF-2 and MOF-5 discussed above illustrated the power of the SBU approach in creating stable porous MOF structures and served as the turning point in the field. Since then, a wide variety of different polynuclear clusters have been used as SBUs. MOF chemistry is, however, not limited to SBUs known from molecular chemistry; SBUs that have no molecular counterpart, such as large ring-shaped $Al_8(OH)_8(HCOO)_4(-COO)_{12}$ (16) and $Be_{12}(OH)_{12}(-COO)_{12}$ SBUs (17), and 1D rod SBUs (18) have also been reported. Judicious choice of SBUs and linkers has resulted in MOFs with ultra-high porosity (19, 20). While the metrics of the linker are decisive in achieving large free pore volume, the rigidity of the SBUs is critical in maintaining permanent porosity. The concept of SBUs is also helpful in simplifying and classifying MOF structures in terms of net topology (21). The well-defined geometry and overall connectivity of SBUs play a pivotal role in the a priori synthesis of new MOFs following geometric design principles. The geometrical and chemical variety of SBUs facilitates the formation of a wide range of different structures, while the organic linkers can be used as a tool to control the metrics. Accordingly, the structural richness of MOFs, their properties, and the place they are beginning to occupy in the larger context of chemistry are attributable to the development of the SBU approach. In this contribution, we highlight how SBUs have given rise to (i) permanently porous MOFs, (ii) principles for their design and synthesis, (iii) framework reaction chemistry, and (iv) functional properties (Fig. 1).

A PRIORI SYNTHESIS OF MOFS

The lack of predictability of the structures of solids prepared using traditional synthetic methods is rooted in the fact that there is little to no correlation between the structure of the starting materials and

that of the products. In its greater predictability, MOF chemistry is fundamentally different from that of traditional solid-state materials. Here, reaction conditions have been established under which a certain SBU with a given geometry and overall connectivity forms. In combination with the well-defined structure of the organic linker, this information eliminates the serendipity presented in the realm of coordination networks and other extended solids. Consequently, the SBU approach makes it possible to control the connectivity and geometry of both building units, and thus to target MOFs with predetermined topologies (22). The a priori synthesis of MOFs requires that all the following prerequisites are fulfilled: (i) The chemistry of the metal ion used to form a specific SBU is well understood, and the formation of a specific type of SBU can be predicted. This requirement is important because subtle variations in synthetic conditions may result in the formation of different types of SBU. (ii) The constitution of the organic linker must remain unaltered during synthesis, and its specific functionalities must not interfere with the formation of the targeted SBU. (iii) The reaction conditions must allow reversible framework formation, error correction, and, consequently, the formation of an ordered crystalline material. (iv) No structure-directing agent must be used, and the reticulation of the building units is directed toward their “default” structure by the directionality and rigidity inherent to the individual building units.

The design of MOFs with predetermined topologies begins by determining the chemical building units required to construct the selected net in a process termed “reticular synthesis.” This design process includes determination not only of the connectivity of individual building units, but also of the exact geometry dictated by the local symmetry of the positions they occupy in the targeted net. With respect to net topologies, we refer to building units with two points of extension as “links” and to those with three or more points of extension as “nodes.” These links and nodes are assembled into the simple net, which does not distinguish between vertices of identical connectivity but different geometry. These differences and the concomitant restriction with respect to the angles and distances within and between the building units are part of the augmented net. For a given set of building units, the edge-transitive nets are the most likely ones to form, and these are referred to as the “default topology.” In Fig. 2, all edge-transitive nets for binary combinations of linker and SBU geometries frequently encountered in MOF chemistry are shown in their augmented form, and possible non-edge-transitive nets are listed in the light gray boxes. This illustration gives credence to the claim that the structural diversity encountered in MOF chemistry originates largely from the wide variety of accessible SBU geometries and that, by choosing appropriately shaped and sized building units, it is possible to target certain structures. These topological considerations imply that the reticulation of building units of the same geometry and connectivity but different metrics leads to “isoreticular” frameworks, meaning frameworks of the same topology, but altered metrics or functionality (23).

The “isoreticular principle” provides a powerful conceptual framework for expanding pore size while maintaining the underlying topology of the MOF and, to a certain degree, their pre-synthetic isoreticular functionalization. The isoreticular expansion and functionalization of MOFs was first reported for MOF-5 (23). It was shown that, using expanded linear ditopic linkers, isoreticular expanded analogs of MOF-5 can be prepared with pore diameters up to 28.8 Å [IRMOF-16, $Zn_4O(TPDC)_3$; TPDC = [1,1':4',1''-terphenyl]-4,4''-dicarboxylate]. In a manner akin to that described above,

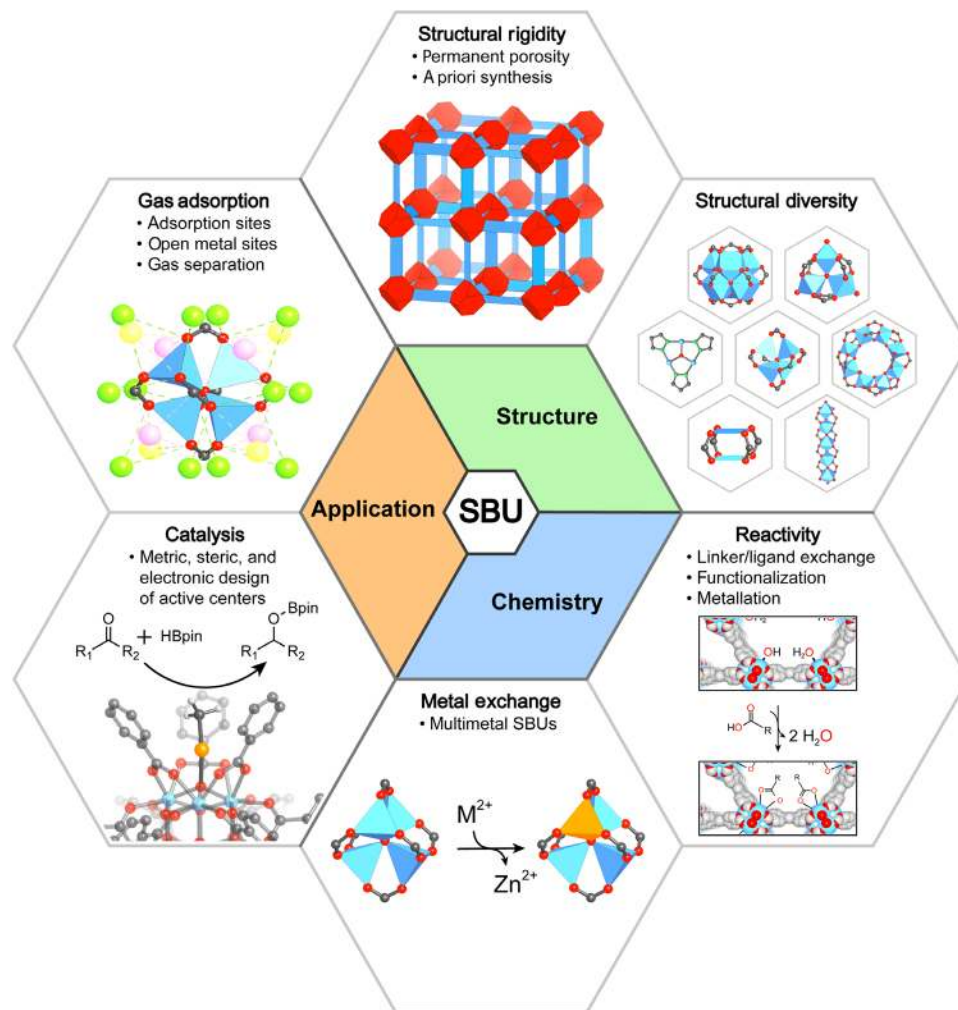


Fig. 1. Impact of the SBU on the structure, chemistry, and applications of MOFs. The rich structural chemistry of MOFs is founded on the structural diversity of the SBUs. Furthermore, the structural rigidity of the SBUs renders MOFs mechanically and architecturally stable, and thus permanently porous. The chemical nature of SBUs gives rise to “framework chemistry”—the post-synthetic chemical modification of MOFs—and is key to further extending their applications. Chemical modifications include substitution reactions of linkers and terminal ligands, metallation reactions, and metal ion exchange reactions. Prominent applications of MOFs that profit from the chemical nature of the SBU are gas and vapor adsorption, separations, and catalysis.

functionalized linkers bearing $-NH_2$, $-Br$, $-OR$ ($R = C_3H_7, C_4H_9$) groups were used to prepare isoreticular functionalized MOF-5 analogs. The isoreticular principle is generally applicable and provides the potential to target macroscopic pore sizes in a rational manner. The stability of isoreticular expanded MOFs relies heavily on the rigidity of the SBU and the concomitant architectural stability of the framework. The expansion of the H_3BTC (benzene-1,3,5-tricarboxylic acid) linker used to prepare MIL-100 $\{[M_3O(H_2O)_2L](BTC)_2; L = OH, F\}$ (24) was reported to yield isoreticular analogs with up to 68 Å large cages $\{PCN-333, [M_3O(H_2O)_2L](TATB)_2; TATB = 4,4',4''-(1,3,5\text{-triazine-2,4,6-triyl})tribenzoic\}$ (25), and 85 × 98 Å large pores were reported for isoreticular expanded MOF-74 analogs $[IRMOF-74\text{-XI}, Mg_2(DOT\text{-XI})]$ (26), marking the largest 3D and 1D pores in MOFs reported today.

There are several examples where more than one edge-transitive net exists for a given set of identical building units. In these cases, the maximum symmetry embedding and the topological density provide information on which structure is more likely to form. One

such example is the reticulation of 8-c Zr_6O_8 core SBUs and tetraprotic $H_4TCPP-H_2$ [tetra(*p*-carboxyphenyl)porphyrin] linkers that can lead to frameworks of **csq** (maximum symmetry embedding $P6/mmm$, No. 191, transitivity 2155), **sqc** (maximum symmetry embedding $P4_1/amd$, No. 141, transitivity 2132), or **scu** (maximum symmetry embedding $P4/mmm$, No. 123, transitivity 2133) topology depending on whether the reaction is carried out under thermodynamic or kinetic control. Under thermodynamic control (that is, high temperatures and strong modulator), a **csq** framework $[MOF-545, Zr_6O_4(OH)_4(TCPP-H_2)_2(H_2O)_4(OH)_4]$ is formed (27), a framework of **scu** topology $[NU-902, Zr_6O_4(OH)_4(TCPP-H_2)_2(H_2O)_4(OH)_4]$ is the kinetic product formed under mild conditions (that is, low temperature and weak modulator) (28), and an **sqc** topology framework $[PCN-225, Zr_6O_4(OH)_4(TCPP-H_2)_2(H_2O)_4(OH)_4]$ is formed at intermediate temperatures using an intermediate modulator (29).

Another case is the formation of nets of the same connectivity from building units of the same general geometry but different chemical composition. Here, subtle changes in the pK_a and geometric








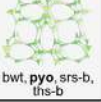
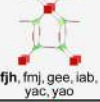

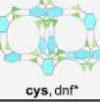


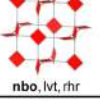
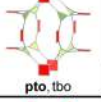
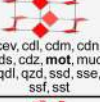
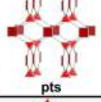
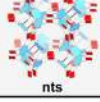
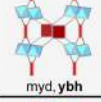

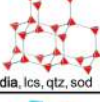
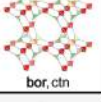
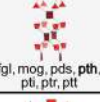
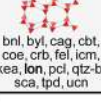
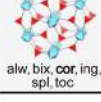

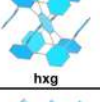
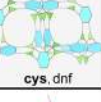
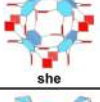
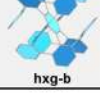

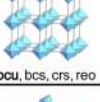
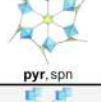
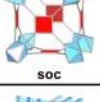
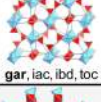
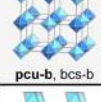

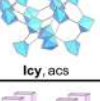

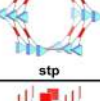
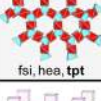
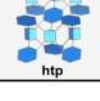
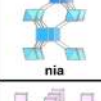
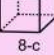
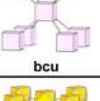
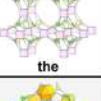
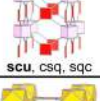
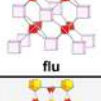
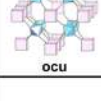

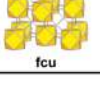
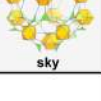
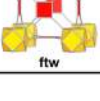
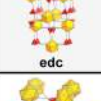

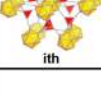
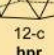
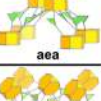
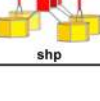

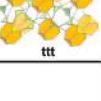
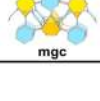

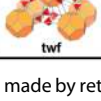
Building unit 1 \ Building unit 2	— 2-c Linear	 3-c Triangle	 4-c Square	 4-c tet	 6-c Hexagon	 6-c oct
 3-c Triangle	 srs	 bwt, pyo, srs-b, ths-b	 fjh, fmj, gee, iab, yac, yao	 asn, ept, ofp	 cys, dnf*	 anh, ant, apo, brk, cep*, cml, czz, eea, qom, rti, tsx, zzz
 4-c Square	 nbo, lvt, rhr	 pto, tbo	 cev, cdl, cdm, cdm, cds, cdz, mot, muo, qdl, qzd, ssd, sse, ssf, sst	 pts	 nts	 myd, ybh
 4-c tet	 dia, lcs, qtz, sod	 bor, ctn	 fgl, mog, pds, pth, pli, ptr, ptt	 bni, byl, cag, cbt, coe, crb, fel, icm, kea, lon, pci, qtz-b, sca, tpd, ucn	—	 alw, bix, cor, ing, spl, toc
 6-c Hexagon	 hxg	 cys, dnf	 she	—	 hxg-b	—
 6-c oct	 pcu, bcs, crs, reo	 pyr, spn	 soc	 gar, iac, ibd, toc	—	 pcu-b, bcs-b
 6-c trp	 lcy, acs	 ceq, dag, fmz, hwx, moo, sab, sit, ydq	 stp	 fsi, hea, tpt	 htp	 nia
 8-c cub	 bcu	 the	 scu, csq, sqc	 flu	—	 ocu
 12-c cuo	 fcu	 sky	 ftw	 edc	—	—
 12-c ico	—	—	—	 ith	—	—
 12-c hpr	—	 aea	 shp	—	—	—
 12-c tte	—	 ttt	—	—	 mgc	—
 24-c tro	—	—	—	 twf	—	—

Fig. 2. The reticular table. A table of possible bipartite nets representing binary frameworks made by reticular chemistry. All topologies are shown as their corresponding augmented net. If more than one net exists, then the identifier of the indicated net is shown in bold. In these cases, either the local symmetry of the building units (for example, torsion angles and dihedral angles) or the comparison of the maximum symmetry embedding and the topological density helps to decide which net is most likely to form from the given set of building units. The edge-transitive nets are the most likely products of reticular synthesis and are shown on a white background. The light gray fields indicate possible non-edge-transitive nets for a given combination of building units. All identifiers are given in alphabetical order. All data shown are taken from the Reticular Chemistry Structure Resource (23 March 2018) (110) and were collected using the search routines for the respective combination of vertices.

constraints of either building unit can direct the synthesis toward one topology or the other; however, these effects are difficult to predict. An additional factor influencing the formation of one topological isomer over the other is the topological density. Because nature does not like open space, for topological isomers of identical transitivity and an identical/similarly symmetric maximum symmetry embedding (for example, **ctn** and **bor**), the topology with the higher topological density is the one more likely to form.

COMPLEXITY ARISING FROM MULTIPLE SBUS

The ability to deliberately target the formation of specific types of SBU by judicious choice of starting materials and precise adjustment of the reaction conditions makes it possible to design and synthesize MOFs with structures that contain multiple SBUs. Four approaches have been reported, including mixed-metal SBUs, mixed SBUs in a single MOF, tertiary building units (TBUs), and the post-synthetic incorporation of additional SBUs.

The mixed-metal approach represents the simplest case. Here, all SBUs are of the same general type (composition, geometry, and connectivity), but are constructed from more than one kind of metal ion. An example of this approach is an isorecticular series of mixed-metal multivariate MOFs of the general formula $[M_3OL_3]_2(TCPP-M/H_2)_3$ (Fig. 3A) (30). All MOFs of this series are constructed from the same trinuclear $[M_3OL_3](-COO)_6$ SBU and tetratopic porphyrin-based linker. A combination of five different metals and six different linkers (unmetallated TCPP- H_2 and five metallated derivatives TCPP-M) was used to prepare a total of 36 isostructural MOFs. With respect to the distribution of different metals within these structures, two scenarios can be envisioned as follows: (i) the formation of domains containing SBUs that are composed of one kind of metal and (ii) a well-mixed scenario, where mixed-metal SBUs are formed and randomly distributed throughout the crystal. It was found that metals of similar radius and electronegativity tend to form mixed-metal SBUs (that is, the well-mixed scenario), and metals that have significantly different radii and electronegativity result in the domain scenario.

A further increase in structural complexity is realized by combining more than one type of SBU within one MOF structure following the “multi-SBU approach.” Simple examples include the substitution of linkers by SBUs of the same local symmetry. The **tbo** framework MOF-325 $\{Cu_3(H_2O)_3[(Cu_3O)(PyC)_3(NO_3)_2]_2\}$; PyC = 4-pyrazolecarboxylate (31) is isorecticular to HKUST-1 $[Cu_3(BTC)_2]$ (15). Here, the trigonal planar BTC linkers in HKUST-1 have been replaced by trigonal planar $Cu_3OL_3(PyC)_3$ moieties, thus giving rise to a complex expanded analog that is built from two different types of SBU. Similarly, the tritopic BTB linker in MOF-205 $\{(Zn_4O)_3(BTB)_4(NDC)_3\}$; BTB = 5'-(4-carboxyphenyl)-[1,1':3',1''-terphenyl]-4,4''-dicarboxylate and NDC = naphthalene-2,6-dicarboxylate (19) can be replaced by $Cu_3OL_3(PyC)_3$ moieties, resulting in the formation of FDM-7 $[(Zn_4O)_3(Cu_3(OH)_4(PyC)_3)_4(NDC)_3]$ (Fig. 3B) (32). In FDM-7, the two distinct SBUs are not only of different connectivity (6 and 3, respectively) and geometry (octahedral and trigonal, respectively) but also are built from two different metals (zinc and copper, respectively). The interesting redox chemistry of $(Cu^{2+})_3(\mu-OH)(OH)_3(PyC)_3$ SBUs, which can be reversibly reduced to give $(Cu^{1+})_3(PyC)_3$, makes these materials interesting catalysts for oxidation reactions (32). The combination of $Zn_4O(-COO)_6$ and $Cu_3OL_3(PyC)_3$ -type SBUs gives rise to a myriad of different structures, including those that cannot be accessed in the simpler binary systems (32, 33). Using the multi-

SBU approach, MOFs with up to seven distinct SBUs have been prepared (33), highlighting the importance of this approach in expanding the scope of accessible structure types.

Linking large TBUs with predetermined geometry and connectivity into extended structures provides yet another opportunity for the design and synthesis of complex MOFs. Metal-organic polyhedra (MOPs) (34) constitute ideal building units for this approach. Their typically high connectivity not only allows the formation of topologies not accessible by any other approach but also helps to reduce the number of possible topologies for a given set of building units, thus increasing predictability. TBUs are generally formed in situ by linking multiple SBUs through segments of the organic linkers into discrete 0D polyhedra. The SBUs render these molecular entities stable, and the organic linkers that connect adjacent SBUs encode the information for their in situ formation. An early example based on this approach is **rht**-MOF-1 $\{[Cu_2(TZI)_2(H_2O)_2]_{12}[Cu_3O(OH)(H_2O)_2]_8\}$; TZI = tetrazolate-5-(phenyl-3,5-dicarboxylate) (Fig. 3C) (35). The structure of **rht**-MOF-1 is designed by dissecting the H_3TZI linker into an isophthalic acid and a tetrazole segment. Reticulation of Cu^{2+} with isophthalic acid yields MOP-1 $[Cu_2(m-BDC)_2(H_2O)_2]$ (34), a molecular cage of **rco** topology that is built from 24 *m*-BDC units and 12 copper paddle wheel SBUs. This finding predicts that reticulation of Cu^{2+} with H_3TZI should lead to the formation of a MOP-1 derivative bearing 24 tetrazole units and thus providing a 24-c TBU of truncated cuboctahedral shape. Linking these tetrazoles through copper ions in the form of $Cu_3O(OH)(H_2O)_2(tetrazole)_3$ SBUs leads to the formation of the targeted 3,24-connected **rht** framework (Fig. 3C). The trigonal hexatopic $Cu_3O(OH)(H_2O)_2(TZI)_3$ units can be replaced by purely organic trigonal hexatopic linkers of appropriate geometry to give isorecticular frameworks (35–37), among them NU-110E (20), the current record holder for the highest surface area ($S_{BET} = 7140 \text{ m}^2 \text{ g}^{-1}$). Analogous to the examples discussed above, a wide range of different MOPs can be employed in the “TBU approach,” and more detailed reviews of such MOFs are found elsewhere (36, 38, 39).

Recently, the multistep synthesis of a complex MOF structure that contains two different types of SBU has been reported (40). By analyzing the pathway of MOF synthesis, the authors showed that, upon mixing of all starting materials, the thermodynamic product is most likely to form, which, for the case of complex mixtures containing multiple different components, may lead to phase separation. Consequently, to realize the kinetic product, the synthesis was planned in a similar way to that of organic retrosynthesis. The different components were installed in separate steps, where each step results in the thermodynamic product for the respective reaction. The **she** topology framework PCN-224(Ni) $[(Zr_6O_4(OH)_8(H_2O)_4)_4(Ni-TCPP)_6]$; Ni-TCPP = tetra(*p*-carboxyphenyl)porphyrin-Ni(II)] was chosen as a starting point because a maximum of six additional linkers can be attached to its 6-c Zr_6O_8 core SBUs. A theoretical model shows that additional trigonal tritopic linkers of appropriate geometry can bridge adjacent SBUs in PCN-224(Ni) in a way that the third binding group of the additional linker can facilitate the formation of further M_6O_8 core SBUs and thus a framework of **amu** topology. However, no trigonal linker fulfilling the symmetry requirements imposed by the structure of PCN-224(Ni) was found; but it was shown that disordered bent ditopic DCPDS (4,4'-sulfonyldibenzoic acid) features an appropriate geometry. Linker incorporation and subsequent reaction with $HfCl_4$ lead to the formation of PCN-224(Ni)-DCPDS and PCN-202(Ni)-Hf, respectively. PCN-202(Ni)-Hf features a 4,4,7-connected net (**hcz**

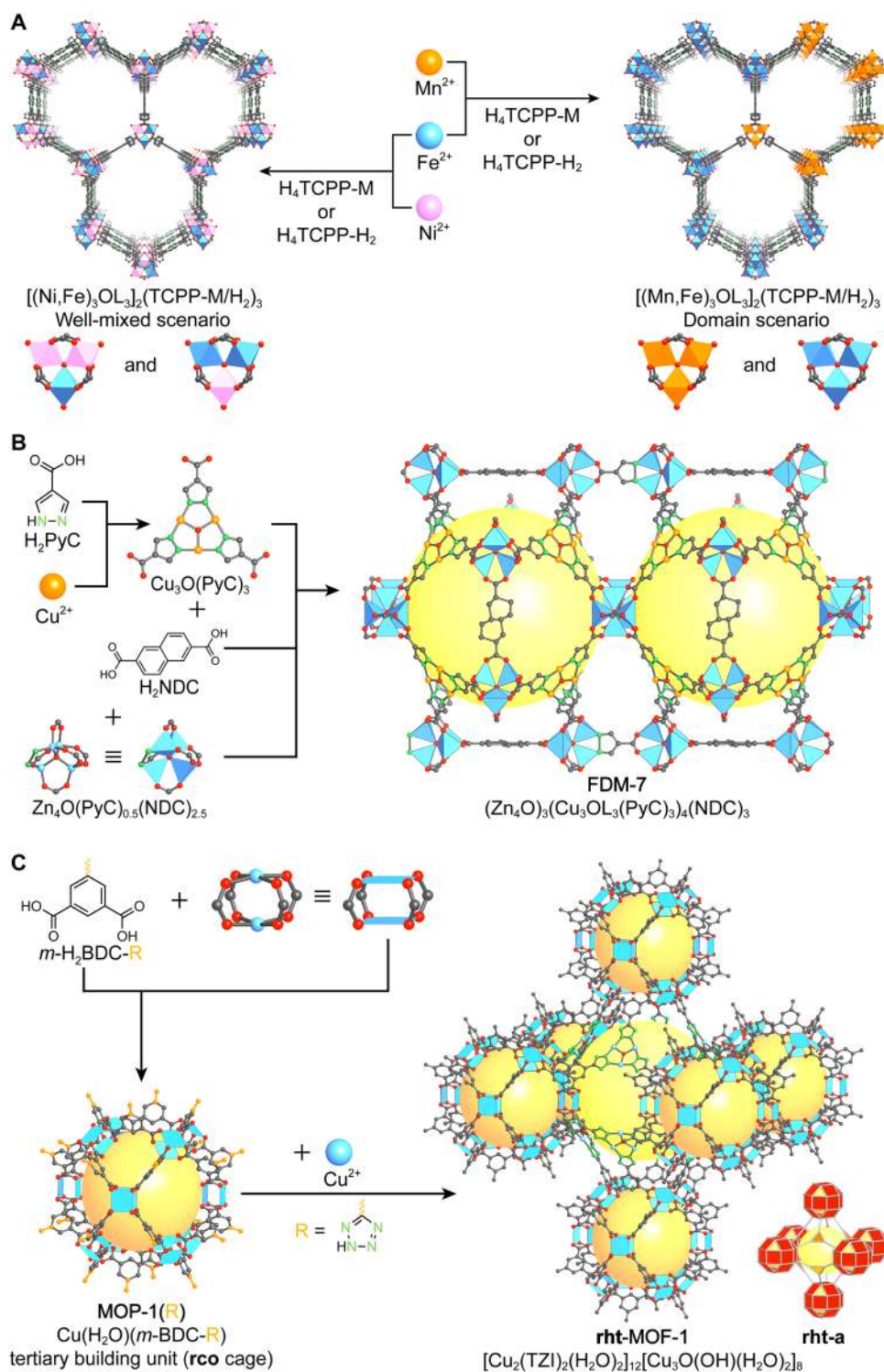


Fig. 3. Complexity in MOFs through the multi-SBU approach. (A) Crystal structure of $[\text{M}_3\text{OL}_3]_2(\text{TCPP-M})_3$ with an underlying **stp** topology. The well-mixed scenario (mixed-metal SBUs; left) is observed for metals with similar radii and electronegativity (for example, Fe^{2+} and Ni^{2+}). In contrast, for metals with significantly different radii and electronegativity (for example, Mn^{2+} and Fe^{2+}), the domain scenario (right) is observed. (B) Crystal structure of FDM-3. The two different binding groups of the PyC linker lead to the formation of octahedral $\text{Zn}_4\text{O}(\text{-COO})_6$ and $\text{Zn}_4\text{O}(\text{-COO})_5(\text{NN})$ SBUs and trigonal $\text{Cu}_3(\mu_3\text{-OH})(\text{OH})_3(\text{PyC})_3$ SBUs, which show interesting redox chemistry. (C) The TBU approach allows the targeted synthesis of highly complex structures. Here, metal-organic polyhedron-1 (MOP-1; **rco**) TBUs are linked by trigonal Cu_3OL_3 (tetrazolate)₃ SBUs to give a MOF of **rht** topology. The formation of the TBU (left) and further linking into an extended structure (right) are shown.

topology) and two distinct SBUs built from two different metals. This rational approach to complex structures requires the additional building units to precisely match the symmetry and metrics of the pockets within the pristine structure, a prerequisite that severely limits the number of appropriate building units compared to a direct synthesis.

FRAMEWORK CHEMISTRY AT THE SBUS

The chemistry of SBUs not only allows the rational design of new MOF structures but also largely defines the thermal (that is, thermodynamic stability of the M–O bond) and chemical (that is, thermodynamic stability of the M–O bond, reduction potential, and kinetic inertness of the metal center) stability of the overall structure. The fact that the bonds between linkers/ligands and the SBUs generally represent the chemically most reactive portion of the framework structure makes the SBUs the center of many post-synthetic modifications (PSMs). The manifold types of modification reactions arise from the possibility of harnessing different types of interaction, ranging from weak coordination bonds to strong and covalent interactions. In the following section, we will discuss selected examples that highlight the importance of these modifications classified by the strength of the interactions involved.

One of the first PSMs carried out on SBUs in MOFs was the creation of open metal sites—coordinatively unsaturated metal centers within the SBUs—by removing neutral terminal ligands (41, 42). This approach is particularly interesting because it is applicable to a wide range of SBUs that bear neutral terminal ligands. Synthetically, open metal sites are generated by heating MOFs that are built from SBUs that bear neutral terminal ligands under dynamic vacuum. Open metal sites feature a large unoccupied orbital, and their Lewis acidic nature gives rise to Lewis acid-base chemistry, high activities in acid-catalyzed reactions, and strong interactions with guest molecules (43). The coordinative functionalization of open metal sites with amines is well studied, and materials with diamines grafted to the open metal sites show interesting properties with respect to catalysis (44) and gas adsorption (45, 46).

Modifications involving strong interactions include the substitution of charged ligands or linkers and the formation of heterometallic SBUs by coordination of additional metals to Lewis basic terminal ligands. The incorporation of ligands into MOFs is commonly referred to as solvent-assisted ligand incorporation (SALI) and is achieved by treating the pristine MOF with an excess of the linker/ligand to be incorporated. This process allows the replacement of terminal ligands by functional molecules of the appropriate size and geometry that bear suitable binding groups. When applied to a chiral framework, molecules can undergo coordinative alignment (CAL) with the framework. Here, the MOF acts as a substrate for the crystallization of organic molecules. The chiral MOF-520 [Al₈(OH)₈(BTB)₄(HCOO)₄, space group *P*4₂2₁2] is an ideal substrate for the CAL method (Fig. 4A) (47). In MOF-520, each octanuclear SBU is connected to 12 BTB linkers and 4 formate ligands that can be replaced by molecules with appropriate binding groups such as carboxylic acids, primary alcohols, and 1,2-diols. Aligning molecules in this way was shown to facilitate the discrimination of single and double bonds, and the non-centrosymmetric framework serves as a reference in the structure solution, enabling the unambiguous assignment of the absolute configuration of the aligned molecule. Ligand exchange reactions facilitate the incorporation of not only organic but also inorganic molecules such as acids. Treatment of MOF-808 [Zr₆O₄(OH)₄(BTC)₂(HCOO)₆] with

aqueous sulfuric acid was reported to lead to partial replacement of the capping formate ligands on the Zr₆O₅(OH)₃(HCOO)₅(H₂O)₂(-COO)₆ SBUs by SO₄²⁻ ions (on average 2.5 SO₄²⁻ per SBU). The resulting MOF termed MOF-808-2.5SO₄ was shown to be a super acid (48).

In a similar fashion, terminal ligands can be exchanged by linkers to give rise to new MOFs that are not accessible by direct synthesis. An example of this kind of process is the topological transformation of PCN-700 {Zr₆O₄(OH)₈(H₂O)₄(Me₂-BPDC)₄; Me₂-BPDC = 2,2'-dimethyl-[1,1'-biphenyl]-4,4'-dicarboxylic acid} (49). The structure of PCN-700 features two distinct pockets between the cubic Zr₆O₄(OH)₈(H₂O)₄(-COO)₈ SBUs that can be bridged sequentially using linkers of appropriate length. This approach not only provides synthetic access to new unusual topologies and mixed linker systems but also can be used as a handle to manipulate the mechanical properties of frameworks, as was reported for the “molecular retro-fitting” of MOF-520 using BPDC ([1,1'-biphenyl]-4,4'-dicarboxylate) girders (Fig. 4B) (50). Introduction of additional BPDC linkers into the structure of MOF-520 (**fon** topology) that connect adjacent SBUs leads to the formation of MOF-520-BPDC (**skd** topology). The BPDC “girders” increase the mechanical stability of MOF-520-BPDC compared to MOF-520, as evidenced by the fact that, in contrast to pristine MOF-520, the more rigid architecture of MOF-520-BPDC prevents its expansion by diffusion of pressure-transmitting medium molecules into the pores when hydrostatic pressure is applied. As a result, no structural degradation of MOF-520-BPDC was observed upon cycled high hydrostatic compression and decompression in a diamond anvil cell at pressures up to 5.5 GPa, whereas amorphization of MOF-520 was reported at pressures lower than 3 GPa.

Topological transformations can be realized not only by implementation of additional linkers into, but also by controlled removal of linkers from, a MOF structure. Removal of one quarter of the Zn²⁺ ions and half of the PyC linkers from the **pcu** framework Zn₄O(PyC)₃ results in a transition into a cationic **srs** topology framework of chemical formula [Zn₃□(OH)(PyC)_{1.5}□_{1.5}(OH)(H₂O)_{3.5}](PyC)_{0.5} (where □ = vacancy) with ordered vacancies (Fig. 4C) (51). The original **pcu** topology can be restored by filling these vacancies using additional R-H₂PyC linkers and suitable metal ions (for example, Li⁺, Co²⁺, Cd²⁺, and La³⁺). In this way, structures with an ordered spatial arrangement of functionalized linkers and metal constituents can be realized. These exchange reactions are made possible by the structural robustness of the **srs** intermediality imparted by the rigid SBUs.

The outstanding mechanical and architectural stability imparted by the SBUs allows the replacement of terminal/capping ligands by other ligands or linkers, as well as the exchange of linkers within the structure. These reactions have been intensively studied for UiO-66 [Zr₆O₄(OH)₄(BDC)₆], an **fcu** topology framework built from 12-c Zr₆O₈ core SBUs connected by linear ditopic BDC linkers. Replacement of the BDC linkers by functionalized derivatives such as NH₂-BDC, Br-BDC, N₃-BDC, OH-BDC, and (OH)₂-BDC was reported to occur in high yields (52). In some cases, linker exchange reactions have been used to afford the formation of isorecticular expanded MOFs. These reactions have been reported for bio-MOF-100 [Zn₈O₂(AD)₄(BPDC)₆], a triply cross-linked **lcs** framework built from Zn₈O₂(AD)₄(-COO)₁₂ SBUs of truncated tetrahedral shape and linear ditopic BPDC linkers (53). The BPDC linkers in bio-MOF-100 are readily replaced by longer linear ditopic linkers {that is, ABDC = (*E*)-4,4'-(diazene-1,2-diyl)dibenzoic acid and NH₂-TPDC = 2'-amino-[1,1':4',1''-terphenyl]-4,4''-dicarboxylic acid} to give the

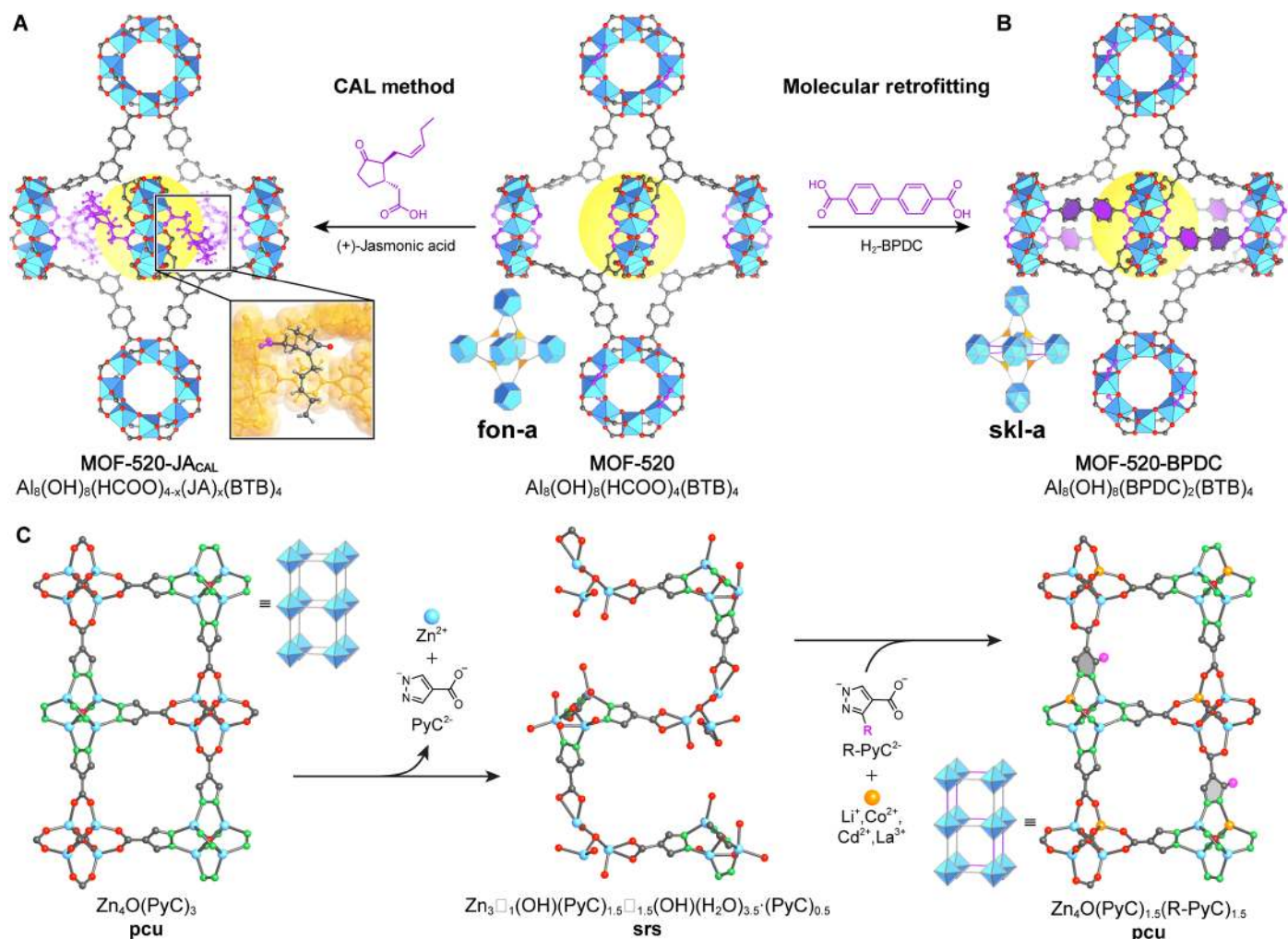


Fig. 4. Ligand and linker exchange reactions in MOFs. (A) The capping formate ligands on the octanuclear $\text{Al}_6(\text{OH})_8(\text{HCOO})_4(-\text{COO})_{12}$ SBUs can be exchanged with molecules bearing appropriate binding groups. Here, the alignment of (+)-jasmonic acid is shown. The chiral framework serves as a reference for the determination of the absolute configuration of the aligned molecule by x-ray crystallography. (B) In a similar manner, the capping formate ligands can be replaced by linear ditopic BPDC linkers to afford a transformation of the **fon** topology (MOF-520) into the **skl** topology (MOF-520-BPDC). MOF-520-BPDC exhibits enhanced mechanical stability compared to pristine MOF-520. (C) The architectural stability provided by the SBUs allows the formation of ordered vacancies, as exemplified by the topological transformation of the **pcu** topology framework $\text{Zn}_4\text{O}(\text{PyC})_3$ into the **srs** framework $[\text{Zn}_3\text{O}(\text{OH})(\text{PyC})_{1.5}\text{O}(\text{H}_2\text{O})_{3.5}(\text{PyC})_{0.5}]$. Addition of metal ions and linkers regenerates the **pcu** framework, and by using functionalized linkers, an ordered arrangement of functionalities can be realized.

isorecticular expanded analogs bio-MOF-102 and bio-MOF-103 in single-crystal to single-crystal transformations (54). An isorecticular expansion like this is made possible by the triply cross-linked structure, a feature that can only be realized in frameworks based on SBUs.

The polynuclear structure of the SBUs also makes it possible to exchange one or more of their metallic constituents without altering the overall structure of the framework. This phenomenon is well known in geology, as minerals are rarely of pure phase because often foreign ions of similar size and charge are incorporated into the host structure. Metal ion exchange reactions have been reported for many different types of SBU, and they enable the formation of MOFs that are not accessible by direct synthesis (55). However, thus far, no conceptual framework for using metal ion exchange as a general method has been established, and only rough guidelines have been proposed: (i) SBUs that undergo cation exchange are often coordinatively unsaturated. (ii) SBUs built from coordinatively saturated metals can

undergo metal ion exchange reactions if the M–O bonds are thermodynamically unstable or kinetically labile. (iii) The structure of the pristine MOF may influence the rate of ion exchange. This is mainly related to the ease of structural deformation during the exchange process. (iv) Periodic trends of metal ion exchange are not fully established; however, experimental observations indicate that Cu^{2+} ions replace most other second-row transition metals and that Mn^{2+} , Cd^{2+} , and Pb^{2+} show higher exchange rates than Cu^{2+} (55). Such exchange reactions have been studied for the $\text{M}_2(-\text{COO})_4$ paddle wheel SBU, showing a trend parallel to the stability of Irving-Williams series (56). Early examples of metal exchange reactions highlight the importance of rigorous characterization of the reaction products to ensure that metal ion exchange has in fact taken place. Soaking UiO-66 in an *N,N'*-dimethylformamide (DMF) solution containing a Ti^{4+} or Hf^{4+} salt was initially reported to lead to the formation of mixed-metal SBUs by partial exchange of zirconium in the $\text{Zr}_6\text{O}_4(\text{OH})_4(-\text{COO})_{12}$

SBUs (57). It was, however, later shown that metal ion exchange does not occur, but a metal oxide coating of titanium and hafnium, respectively, is formed (58). This may be ascribed to the strong M^{4+} -O bonds in $Zr_6O_4(OH)_4(-COO)_{12}$ SBUs, and metal ion exchange reactions are more likely to occur in SBUs with weaker M-O bonds. The replacement of Zn^{2+} ions in the SBUs of MOF-5 by a wide range of different metals including many redox-active di- and trivalent first-row transition metals to give MOF-5 analogs with SBUs containing Ti^{3+} , V^{2+} , V^{3+} , Cr^{2+} , Cr^{3+} , Mn^{2+} , and Fe^{3+} was reported (59). These MOFs are not accessible by typical synthetic pathways. The synthetic approach is identical to that described above; pristine MOF-5 is soaked in concentrated DMF solutions of an appropriate metal salt for an extended period of time. In this way, it was proven possible to create unique coordination environments for the incorporated metal ions that cannot be realized in molecular complexes, making these MOFs interesting candidates for the application in catalysis such as the activation of NO. Substitution following this principle is always incomplete. Quantitative metal ion exchange was reported using a method termed “post-synthetic ion metathesis and oxidation.” Here, the metal ions in MOFs with labile M-O bonds are exchanged with kinetically labile low oxidation state metal ions that are subsequently oxidized, thus driving the reaction to completion (60). These exchange reactions are often realized in single-crystal to single-crystal transformations and therefore can be used for the synthesis of single crystals of MOFs that are otherwise obtained as powders such as Cr^{3+} MOFs.

Besides metal exchange reactions, additional metal ions can be coordinatively bound to the SBU, resulting in heterometallic clusters that often exhibit interesting properties with respect to catalysis. These modifications require the presence of terminal Lewis basic ligands that can coordinate to additional metal ions in a bridging fashion. NU-1000 [$Zr_6(\mu_3-O)_4(\mu_3-OH)_4(H_2O)_4(OH)_4(TBAPy)_2$; TBAPy = 4,4',4'',4'''-(pyrene-1,3,6,8-tetrayl)tetrabenzoic acid], a **csq** topology MOF built from rectangular TBAPy linkers and 8-c Zr_6O_8 core SBUs, has been proven to be an ideal platform for this type of functionalization termed AIM [atomic layer deposition (ALD) in a MOF] due to its high thermal stability and 30 Å large 1D mesopores. Activation of NU-1000 with a mixture of DMF/conc. HCl_{aq} (36:1, v/v) at 100°C facilitates the removal of capping ligands and generates spatially isolated terminal -OH₂/-OH ligands that can subsequently be modified using the AIM method (61). When treated with $Al(CH_3)_3$ or $In(CH_3)_3$, these terminal ligands bind to aluminum and indium under release of two molecules of methane per additional metal ion. These reactions can be carried out using other metals, thus enabling the preparation of a wide range of heterometallic SBUs following this approach.

The reactivity of the bridging -OH groups in the SBUs of MOFs is significantly different from that of the terminal -OH groups used for the functionalization by coordination of metal ions. They allow the PSM of the SBUs involving covalent interactions such as silylation reactions. This is achieved by treating the MOF with highly reactive 1,1'-ferrocenediyl dimethylsilane under solvent-free gas-phase conditions, giving yields of up to 25% (62).

APPLICATIONS ORIGINATING FROM SBUS

Recently, the performance of MOFs in gas storage and separation (63), catalysis (64), sensing (65), and drug delivery (66) has initiated intense research. Applications in the respective fields are based on the porosity inherent to MOFs and made possible by the SBU ap-

proach. Aside from porosity, the chemical nature of the SBUs has a strong influence on the performance of MOFs in these applications, and this will be the focus of the following section.

Gas adsorption and separation

The ultra-high porosity of MOFs early on sparked research in gas storage, and efforts to identify gas adsorption sites within these materials were made. X-ray diffraction, inelastic neutron diffraction, Raman measurements, and theoretical studies show that the polar nature of the SBUs leads to strong interactions with adsorbate molecules, and consequently, the major adsorption sites are located in the vicinity of the SBUs (67–69). Further adsorption sites located close to the faces and edges of the linker molecules feature significantly weaker interactions. Gas molecules were shown to be adsorbed more strongly than in carbon-based materials, and both experimental and theoretical data suggest that the strength of the respective interactions can be further enhanced through polarizing centers such as open metal sites. The creation of open metal sites requires rigid SBUs that prevent structural collapse upon creation of these reactive sites. Prominent SBUs featuring open metal sites are shown in Fig. 5A. The impact of open metal sites on the gas adsorption properties of MOFs is most prominent when considering nonpolar gases such as hydrogen and methane (70). HKUST-1 has one of the highest densities of open metal sites and is therefore, with a capacity of 267 $cm^3 cm^{-3}$ at 35 bar and 303 K, one of the best performing materials with respect to methane storage (Fig. 5B) (71). The Lewis acidic open metal sites were shown to interact strongly with Lewis bases such as the oxygen in CO_2 (72). The chemisorption of CO_2 on the open metal sites of Mg-MOF-74 is depicted in Fig. 5C. The distortion of the linear molecular structure of CO_2 indicates strong interaction with the open metal sites. While open metal sites provide strong polar adsorption sites, they lack selectivity, which poses a problem when attempting CO_2 capture from post-combustion flue gas where both water and CO_2 are present (73).

Inspired by aqueous ethanolamine solutions used for selective CO_2 capture (74), several attempts have been made to functionalize the open metal sites in MOFs with organic diamine species to mitigate the water problem (45, 46, 75). Functionalization of the open metal sites in $Mg_2(DOBPDc)$ (DOBPDc = 4,4'-dioxidobiphenyl-3,3'-dicarboxylate), a MOF isorecticular to MOF-74, with *N,N'*-dimethylethylenediamine (*mmen*) results in a material that shows a step-shaped Type V CO_2 adsorption isotherm. Varying the adsorption temperature was reported to allow for a shift in the inflection point, a phenomenon that enables a large working capacity under temperature swing adsorption (TSA) conditions (76). An adsorption mechanism explaining this unusual behavior was described: CO_2 inserts into the metal-amine bond rather than binding at the terminal amine. Simultaneously, the neighboring amine group deprotonates the amine involved in the insertion step, thereby forming an ammonium carbamate ion pair. The electrostatic interactions stretch the *mmen* species and thus facilitate insertion of the next CO_2 molecule. As a result, an ammonium carbamate chain is formed cooperatively along the rod-SBUs, resulting in a steep step-shaped isotherm (Fig. 5D) (75).

Another strategy for selective adsorption of CO_2 is the modification of SBUs with capping monodentate hydroxyl moieties that bind CO_2 in the form of bicarbonates. This type of functionalization has been reported for two isorecticular triazolate-based frameworks: MAF-X25 and MAF-X27 $\{(M^{2+})_2Cl_2(BBTA); M = Mn \text{ and } Co,$

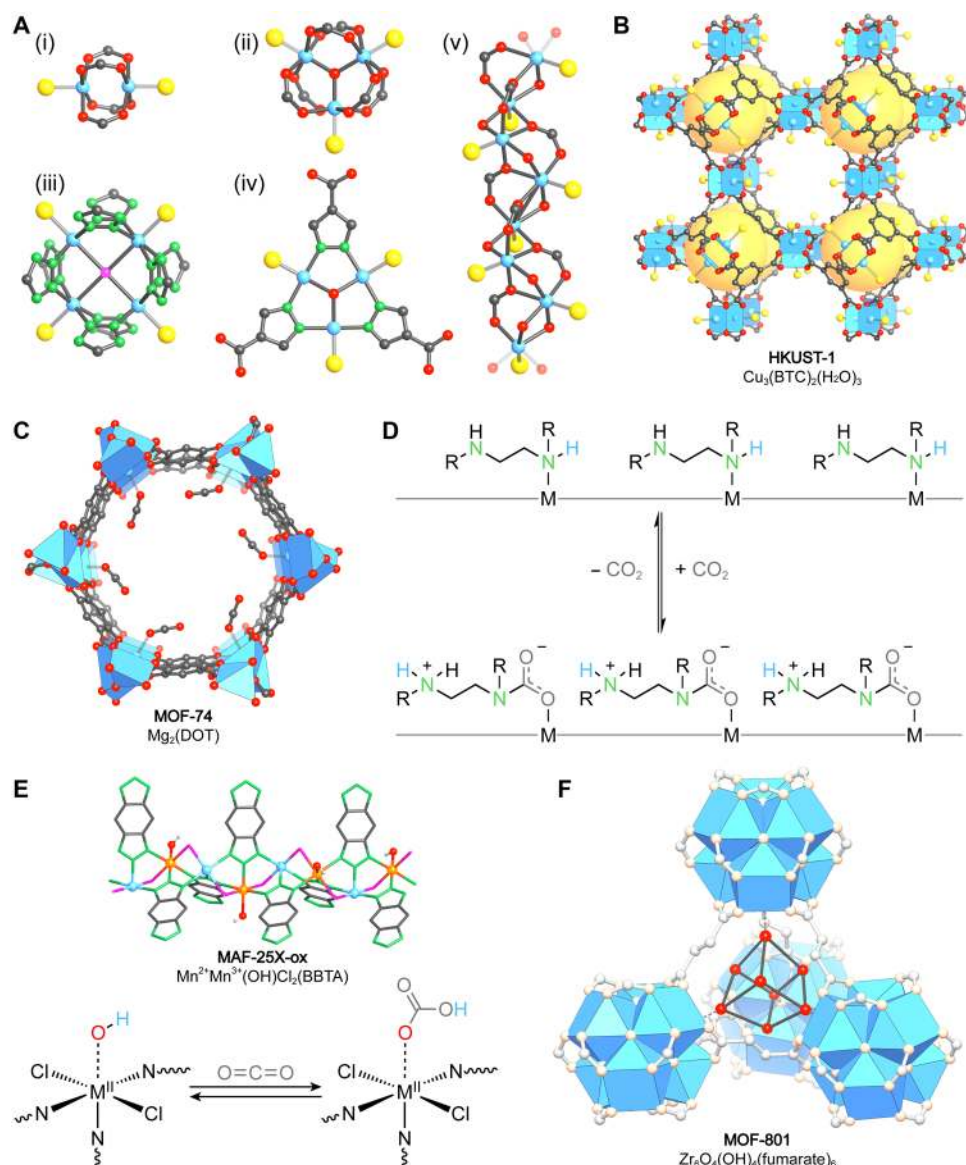


Fig. 5. Adsorption on SBUs. (A) Selection of SBUs with potential open metal sites. (i) $M_2L_2(-COO)_4$, (ii) $M_3OL_3(-COO)_6$, (iii) M_4L_4Cl (tetrazolate) $_6$, (iv) $Cu_3OL_3(PyC)_3$, and (v) $[M_3[O_3(-COO)_3]]_\infty$. These sites feature large unoccupied orbitals that can interact strongly with adsorbent molecules and are commonly generated by heating the MOF in dynamic vacuum. (B) Crystal structure of HKUST-1. The **tbo** framework features one of the highest densities of open metal sites in MOFs; consequently, HKUST-1 has one of the highest methane storage capacities among all MOFs. (C) CO_2 adsorption on the open metal sites in MOF-74. The polarizing nature of the open metal sites leads to a high selectivity for CO_2 over N_2 . Strong interactions are evidenced by the nonlinear geometry of CO_2 in the chemisorbed state. (D) Adsorption of CO_2 in *mmen*- Mg_2 (DOB-PDC) following a cooperative insertion mechanism that allows adsorption-desorption cycles to be realized under mild TSA conditions. (E) Covalent capture of CO_2 on the -OH functionalized SBUs of MAF-X25-ox as bicarbonate. This adsorption mechanism facilitates both a high capacity and a high selectivity for CO_2 . (F) Adsorption of water in the tetrahedral pore of MOF-801. The bridging μ_3 -OH groups of the $Zr_6O_4(OH)_4(-COO)_6$ SBUs act as primary adsorption sites by hydrogen bonding.

respectively; BBTA = benzo[1,2-*d*:4,5-*d'*]bis([1,2,3]triazole)-1,5-diide}. Both MOFs are built from rod SBUs that are connected by BBTA linkers to form 1D hexagonal channels running along the crystallographic *c*-axis (77). Oxidation of the Mn^{2+} centers in the SBUs of MAF-X25 was realized by treatment with H_2O_2 , yielding the -OH functionalized MAF-X25-ox [(Mn^{2+})(Mn^{3+})(OH)Cl $_2$ (BBTA)]. Oxidation of MAF-X25 was shown to increase the CO_2 adsorption capacity by up to 50% due to the change in the adsorption mechanism from chemisorption on open metal sites to covalent binding as bicarbonate (Fig. 5E). This adsorption mechanism was also shown to

be beneficial for the CO_2/N_2 selectivity under dry and wet flue gas conditions.

The chemical nature of SBUs gives rise to different types of interactions with adsorbent molecules, such as hydrogen bonding, π - π stacking, van der Waals, and electrostatic interactions that can afford high selectivity in thermodynamic separation processes. In contrast to the separation of mixtures of chemically dissimilar components (for example, CO_2/N_2), the separation of chemically and physically similar components requires strong and specific adsorbate/adsorbent interactions. Open metal sites provide not only strong adsorption

sites but also the prospect of tuning the selectivity of these sites using different metals to construct the SBUs. This feature has proven to be especially useful in the separation of olefin/paraffin mixtures (78). High selectivity in the separation of ethane/ethylene and propene/propylene mixtures, separation processes of great industrial importance, has been reported for different members of the M-MOF-74 (M = Mg, Mn, Fe, Co, Ni, Zn) series. Fully activated Fe-MOF-74 demonstrates a strong affinity toward unsaturated hydrocarbons, approaching the stoichiometric quantity expected for the adsorption of one molecule per open metal site. This affinity was explained by a combination of the strong interactions of the carbon-carbon double bond with the soft Fe²⁺ cation and π backbonding, leading to long breakthrough times and a high adsorption selectivity of 13 to 18 (at 318 K) for a mixture of ethylene and ethane calculated by ideal adsorbed solution theory (IAST) (79). While Fe-MOF-74 has the highest selectivity in the separation of ethylene/ethane mixtures among all members of the M-MOF-74 series, Mn-MOF-74 is the most selective in the separation of propylene/propane mixtures, highlighting the importance of the metal species constituting the open metal site (80). Open metal sites have also been used in the separation of mixtures of aromatic molecules. M-MOF-74 (M = Mg, Zn, Fe, Co, Ni, Cu, Zn) was tested in the separation of cyclohexane—an important precursor for Nylon 6 and Nylon 66—from benzene. Mn-MOF-74 shows a higher affinity for aromatic molecules, thus allowing an efficient separation from cyclohexane (81).

Bridging -OH groups of aluminum rod-SBUs have been shown to result in highly selective C2 separation (82). NOTT-300 [Al₂(OH)₂(BPTC); BPTC = biphenyl-3,3',5,5'-tetracarboxylate] has a record IAST selectivity of 48.7 for the separation of ethylene/ethane mixtures. This selectivity has been ascribed to supramolecular interactions of ethylene with the host framework, as evidenced by density functional theory (DFT) calculations and inelastic neutron scattering spectra. The bridging -OH groups, protruding into the 1D square pores of NOTT-300, form hydrogen bonds with the carbon-carbon double bond of ethylene. In contrast, ethane exhibits only weak interactions with the framework, which results in the observed high IAST ethylene-ethane selectivity.

SBUs also play an important role in the adsorption of vapors and, more specifically, the adsorption of water vapor, a process that has recently gained more significance, and several MOFs with high water uptake have been reported (83–86). Altering the chemical composition and structure of the SBU influences the hydrolytic stability by introduction of steric shielding, use of kinetically inert metals, or, to some extent, thermodynamic stabilization (86). Further, primary water adsorption sites are located on the SBU because their polar nature leads to strong dipole-dipole interactions and bridging -OH groups facilitate adsorption by hydrogen bonding (87, 88). Figure 5F shows the cubic water cluster formed in one of the tetrahedral pores of MOF-801 [Zr₆O₄(OH)₄(fumarate)₆]. At low relative humidity (RH), a tetrahedral cluster is formed by hydrogen bonding of water molecules to the μ_3 -OH of the SBUs. This cluster evolves into a cubic cluster at higher RH (87). Similarly, the bridging μ_2 -OH groups in the rod-SBUs of MIL-160 [Al(OH)(FDC); FDC = 2,5-furane-dicarboxylate] represent the primary adsorption site, as determined by grand canonical Monte Carlo calculations (88).

Catalysis

MOFs are considered ideal support materials for homogeneous catalysts that provide the prospect of combining the high selectivity of

molecular catalysts and the high reactivity and recyclability of heterogeneous catalysts (89). Their wide structural, chemical, and metal diversity are ideal characteristics for the preparation of tailored materials and fine-tuning of their structure with respect to selectivity and activity. These features provide additional degrees of freedom with respect to catalyst design not known for traditional support materials such as metal oxides, activated carbon, or zeolites (64).

Many examples of catalytically active MOFs use derivatives of homogeneous catalysts as linkers. Prominent examples of this approach are salen-, porphyrin-, and binaphthyl-based linkers (90). While these catalytically active centers are limited with respect to their structures to what is known in the realm of molecular chemistry, the SBU provides the opportunity to create unusual coordination environments and thus unusual catalytic reactivity. The catalysis of wide range of reactions by the SBUs of MOFs has been reported, including Lewis and Brønsted acid-catalyzed reactions, photocatalytic reactions, and redox reactions (91).

While opportunistic approaches are often applied to discovery and investigation of the catalytic behavior of MOFs, the notion of a priori synthesis and targeted structural modification provides rational approaches for the design of MOFs with the desired catalytic activity. A simple way to achieve this goal is by creating open metal sites. These highly reactive sites are unique to MOF chemistry; no molecular analogs featuring these sites are known, due to their high reactivity that leads to structural distortion and aggregation. Consequently, the opportunity to use open metal sites in Lewis acid-catalyzed reactions was explored early in the development of MOF-mediated catalysis. HKUST-1 was reported to catalyze the cyanosilylation of benzaldehyde and acetone (92). Although the catalyst was labile—due to reduction of the Cu²⁺ species—and achieved only moderate yields, this finding was an important step in the development of catalytically active MOFs. The same concept was later transferred to MIL-101 [(Cr₃X(H₂O)₂O](BDC)₃; X = F, OH]. Much higher activity in the same catalytic reaction and a higher stability were achieved in this system, because of the stronger Lewis acidity and lower redox potential of Cr³⁺ (93).

Recently, the post-synthetic metal ion exchange within the SBUs of MOFs has been proven; this is a powerful method to fine-tune the catalytic properties of MOFs (59). An illustrative example for this approach is the metal ion exchange in MFU-4l {Zn^{Oct}Zn^{Tet}₄Cl₄(BTDD)₃; BTDD = bis(1*H*-1,2,3-triazolo-[4,5-*b*],[4',5'-*i*])dibenzo-[1,4]-dioxin)}. The metal ion exchange derivatives of this MOF have been demonstrated to be catalytically active for several chemical transformations (94–97). The pentanuclear 6-c SBU of MFU-4l is well studied in molecular chemistry. Its structure is built from four tetrahedrally coordinated Zn²⁺ ions (Zn^{Tet}) surrounding one central octahedrally coordinated Zn²⁺ ion (Zn^{Oct}) that are all connected through the triazolate segment of the BTDD linker (Fig. 6A). The Zn^{Tet} centers have been demonstrated to be readily replaceable by other metal cations, whereas the central Zn^{Oct} cannot be exchanged (96). Partial exchange of Zn^{Tet,2+} by Ni²⁺ yields Ni-MFU-4l, which catalyzes the dimerization of ethylene to 1-butene—a key monomer in the industrial production of linear low-density polyethylene used for plastic bags, plastic wraps, and other stretchable thin films. Ni-MFU-4l exhibits a very high turnover frequency of 41,500 hour⁻¹ and a selectivity of > 96% for 1-butene—a higher selectivity than those reported for any hetero- and homogeneous catalysts (95). The dimerization follows the Cossee-Arlman mechanism, as evidenced by isotopic labeling experiments substantiated by DFT calculations (97).

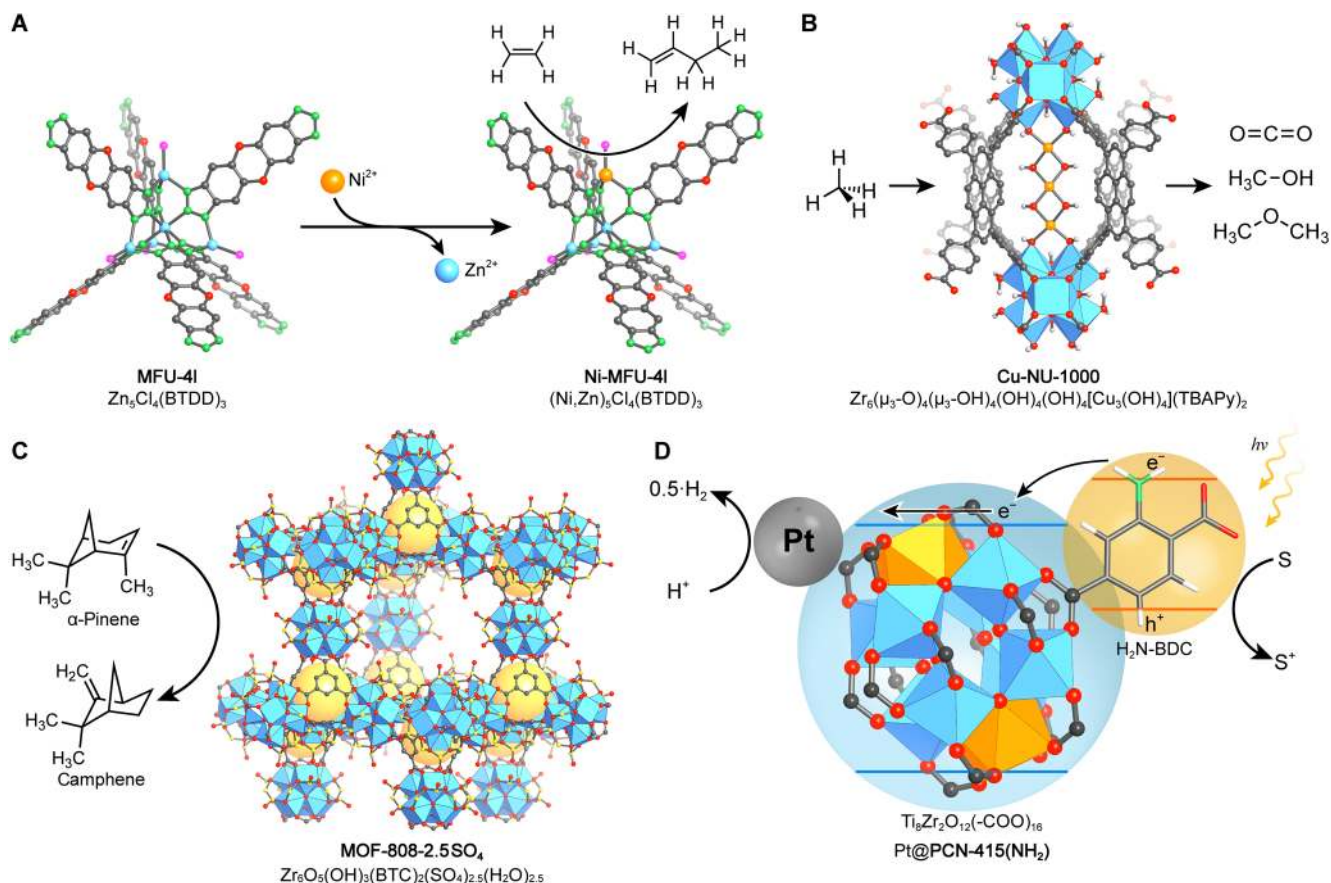


Fig. 6. SBUs as catalytic centers. (A) Cation exchange in MFU-4l generates Ni-MFU-4l, a catalyst for selective conversion of ethylene to 1-butene. (B) Metallation of NU-1000 with copper using the AIM method results in Cu-NU-1000. A Cu-oxo cluster is proposed to form between two Zr-SBUs, which shows high activity for methane oxidation. (C) Immersing MOF-808 in sulfuric acid yields the super acidic MOF-808-2.5SO₄, which was demonstrated to be active in the Brønsted acid-catalyzed isomerization of α -pinene to camphene. (D) Pre-synthesized mixed-metal SBUs provide access to photocatalytically active MOFs such as PCN-415-NH₂. In the presence of TEOA as a sacrificial donor (S), the nanocomposite Pt@PCN-415-NH₂ shows high activity for photocatalytic hydrogen evolution reactions.

Considering the importance of accessible metal centers with respect to catalysis, methods for the selective formation of heterometallic SBUs capable of single-site catalysis have been developed (98, 99). One such strategy is the AIM method, which facilitates the coordination of additional metal centers to terminal -OH groups in zirconium MOFs. The synthesis and catalytic behavior of various AIM derivatives of NU-1000 have been reported (100, 101). Here, Cu-NU-1000 is particularly noteworthy. On the basis of extended x-ray absorption fine structure studies and DFT calculations, the formation of trimeric Cu-oxo clusters bridging adjacent Zr₆O₈ core SBUs was proposed as the predominant copper species formed by AIM (Fig. 6B) (101). Cu-NU-1000 catalyzes the partial oxidation of methane to methanol, with the side products being dimethyl ether and carbon dioxide (Fig. 6B). The desorption of the reaction products was achieved under mild conditions (that is, 135°C) and a stream of 10% water/He (101).

12-c Zr₆O₈ core SBUs cannot be functionalized using the AIM method because of the lack of capping ligands or terminal -OH/-OH₂ groups. Nonetheless, these SBUs can be metallated after deprotonation of the μ_3 -OH groups. Metallation using salts of earth-abundant metals such as CoCl₂ and FeBr₂·THF yields catalysts with a high activity for a wide range of organic reactions (99). Cobalt-metallated UiO-68 [Zr₆O₄(OH)₄(TPDC)₆] was reported to catalyze the site-

selective borylation and silylation of benzylic C-H bonds. The steric environment at the SBUs provides selectivity toward benzylic over aryl functionalization, although the electron-deficient Co²⁺ center should prefer the more electron-rich aryl C-H bonds (99).

Apart from Lewis acidic sites, Brønsted acidity is frequently used in the catalysis of organic transformations. A simple way to introduce Brønsted acidic sites into MOFs is the coordination of protic ligands (for example, water and alcohols) to open metal sites, thus enhancing the polarization of the O-H bond and accordingly also the Brønsted acidity of the respective ligand. This approach entails several disadvantages: The weak coordinative bond is reversible, thus enabling conversion between Brønsted and Lewis acidity. In addition, an excess of the protic ligand can lead to formation of hydrogen bonds and a concomitant decrease in acidity (102). Therefore, the incorporation of larger Brønsted acidic groups by SALI provides a more promising alternative, as was demonstrated for sulfated MOF-808 (Fig. 6C). The degree of substitution was shown to define the acidity of MOF-808-xSO₄, and fully sulfated MOF-808-2.5SO₄ was shown to be a super acid ($H_0 \leq -14.5$) (48). The strong Brønsted acidity was further evidenced by the high activity in the catalytic isomerization of α -pinene to camphene—a reaction that is catalyzed only by strong Brønsted acids, but not by Lewis acids. MOF-808-2.5SO₄ was shown to catalyze further organic transformations,

including Friedel-Crafts acylation, esterification, and isomerization reactions.

The SBUs of carboxylate-based MOFs are structurally related to their respective metal oxide and feature similar electronic properties. In contrast to metal oxides, the spectroscopic properties of MOFs can be tuned by modifications of the linker, rendering them interesting for photocatalysis. In this respect, titanium MOFs are of particular interest because of their photochemistry originating from the titanium-oxo-SBUs. The low radius-to-charge ratio of titanium makes it hard to prepare these MOFs, and therefore, the first titanium MOF, MIL-125 [Ti₈O₈(OH)₄(BDC)₆], was reported as late as 2009 (103)—10 years after the first report of 3D MOFs (14). MIL-125 was shown to catalyze the oxidation of alcohols under nitrogen and exposure to ultraviolet light. In the first step, a Ti³⁺ center is formed by a ligand-to-metal charge transfer (LMCT), which can subsequently be reoxidized to Ti⁴⁺ in the presence of oxygen. The band gap of MIL-125 was shown to be sensitive to additional electron-donating substituents on the BDC linker (104). Appending -NH₂ was demonstrated to shift the LMCT band into the visible region of the electromagnetic spectrum (105). Using this strategy CO₂ could be reduced photocatalytically under visible light irradiation.

Much effort has been made to expand the scope of accessible titanium-based MOFs; however, despite the rich chemistry of titanium clusters, only a few titanium MOFs have been reported at this point (106). The limited success thus far is due to incompatibility of the reaction conditions for the synthesis of these clusters and those required for the crystallization of porous extended framework structures. One approach to mitigating this problem is the reticulation of pre-synthesized functionalized titanium clusters and organic linkers by imine bond formation (107), a strategy well known in the chemistry of covalent organic frameworks (108). Following this approach, two isorecticular MOFs, MOF-901 [Ti₆O₆(OMe)₆(AB)₆(BDA)₃; AB = 4-aminobenzoate and BDA = 1,4-benzenedialdehyde] and MOF-902 [Ti₆O₆(OMe)₆(AB)₆(BPDA)₃; BPDA = 4,4'-biphenyldicarboxaldehyde], were prepared, underpinning the general applicability of this method. Recently, the rational design and synthesis of photocatalytically active MOFs based on pre-synthesized mixed-metal Ti-Zr-SBUs has been reported (109). These authors demonstrated that the capping carboxylate-based ligands of Ti₈Zr₂O₁₂(RCOO)₁₆ (R = Me, Et, Ph, *p*-Tol, and PTBB) clusters are readily replaced by polytopic linkers, which facilitate the formation of MOFs while mitigating the crystallization challenge common to titanium-based MOFs. Using this approach, two isorecticular MOFs [PCN-415, Ti₈Zr₂O₁₂(BDC)₁₂(RCOO)₄; PCN-416, Ti₈Zr₂O₁₂(NDC)₁₂(RCOO)₄] as well as partially [PCN-415(NH₂)_{0.3}, PCN-415(NH₂)_{0.5}, PCN-415(NH₂)_{0.7}], fully [PCN-415(NH₂)], and doubly [PCN-415(2NH₂)] -NH₂ functionalized analogs of PCN-415 were prepared. A composite of Pt nanoparticles and PCN-415-NH₂ was shown to have a high activity in photocatalytic hydrogen evolution reactions. To regenerate the catalyst, a sacrificial donor [triethanolamine (TEOA)] is needed. On the basis of electron paramagnetic resonance and transient absorption spectroscopy studies, the following mechanism for the photocatalytic reaction was proposed: The excitation of the NH₂-BDC linker with visible light leads to a photoexcited electron that is transferred to the Ti⁴⁺ species in a LMCT and subsequently to the Pt nanoparticles that are the catalytically active centers for the hydrogen evolution reaction. Eventually, the oxidized linker is reduced by the sacrificial donor TEOA (Fig. 6D) (109). This elaborate approach to the rational design of MOFs that combine both the structural stability and robustness of zirconium-based MOFs, and

the photocatalytic activity of titanium-based MOFs demonstrates the great advantage of reticular chemistry with respect to functional high-performance materials, and, hopefully, more such synergistic systems will be developed in the future.

OUTLOOK

The use of polynuclear clusters as SBUs in the construction of MOFs has played a pivotal role in realizing chemically and thermally stable, permanently porous extended framework structures. SBUs are also key to the structural diversity inherent to MOFs, and their unique chemistry, as well as to generally applicable principles allowing their design in a rational manner. The accessibility of the pore space in these open framework structures has enabled the exploitation of MOFs for a wide range of applications, including gas storage and separation, harvesting water from air, catalysis, bioimaging, and therapeutics. Fundamentally, both the constituents of MOFs and the space encompassed by them can be used to manipulate matter with a precision previously known only in well-established molecular chemistry. MOFs achieve this capability with full preservation of the crystallinity and porosity of the framework, thus leading to the development of “crystals as molecules.” From a broader point of view, introduction of the SBU approach has helped to extend precision chemistry from molecular complexes and polymers to 2D and 3D frameworks, allowing the rational design of framework structures from functional building units. Recent advances in the synthesis of these frameworks by reticulating pre-designed SBUs and linker molecules confirm the potential of translating properties found in molecular species into framework structures, where they may be amplified and enhanced by synergistic effects and the porous nature of the resulting construct. These properties include, among others, linear and nonlinear optical properties, magnetism, conductivity, and catalysis. Recent advances in computational chemistry will not only help to understand the properties of these materials but also provide means for the prediction of structures with targeted properties. These methods have already been used for the prediction of framework structures with outstanding gas storage capacity, and we expect to see a growing number of reports with even more accurate structure and property predictions in the future.

Incorporation of complexity and heterogeneity within MOFs has been recently reported, and the exploration and analysis of their impact on the structure and property of MOFs have yet to be carried out. Both concepts—heterogeneity and complexity—allow further expansion of the scope of accessible structures and provide access to materials with great potential for increased performance. We envision that controlling the spatial distribution of different organic functionalities and metal ions will lead to the ability to design sequences within or along the MOF backbone, similar to those found in large biomolecules. These specific spatial arrangements of building units will be achieved by integrating multiple different SBUs with specific binding patterns into a single material to direct framework formation or via post-synthetic methods. The realization of this vision will give rise to sequence-dependent materials; we hope that specific sequences can be designed into MOFs to carry out specific functions, and that these functions can operate in sequence as well as in parallel, a feature of special interest with respect to catalysis. The introduction of the SBU marks the turning point in the development of MOF chemistry and will continue to play a key role in their further development, especially for accessing novel structures, properties, and applications.

REFERENCES AND NOTES

1. A. Stein, S. W. Keller, T. E. Mallouk, Turning down the heat: Design and mechanism in solid-state synthesis. *Science* **259**, 1558–1564 (1993).
2. O. M. Yaghi, M. O’Keeffe, M. Kanatzidis, Design of solids from molecular building blocks: Golden opportunities for solid state chemistry. *J. Solid State Chem.* **152**, 1–2 (2000).
3. O. M. Yaghi, M. O’Keeffe, N. W. Ockwig, H. K. Chae, M. Eddaoudi, J. Kim, Reticular synthesis and the design of new materials. *Nature* **423**, 705–714 (2003).
4. R. E. Morris, Modular materials from zeolite-like building blocks. *J. Mater. Chem.* **15**, 931–938 (2005).
5. P. Z. Moghadam, A. Li, S. B. Wiggin, A. Tao, A. G. P. Maloney, P. A. Wood, S. C. Ward, D. Fairen-Jimenez, Development of a Cambridge Structural Database subset: A collection of metal–organic frameworks for past, present, and future. *Chem. Mater.* **29**, 2618–2625 (2017).
6. Y. Kinoshita, I. Matsubara, T. Higuchi, Y. Saito, The crystal structure of bis(adiponitrilo) copper(II) nitrate. *Bull. Chem. Soc. Jpn.* **32**, 1221–1226 (1959).
7. B. F. Abrahams, B. F. Hoskins, D. M. Michail, R. Robson, Assembly of porphyrin building blocks into network structures with large channels. *Nature* **369**, 727–729 (1994).
8. B. F. Hoskins, R. Robson, Design and construction of a new class of scaffolding-like materials comprising infinite polymeric frameworks of 3D-linked molecular rods. A reappraisal of the Zn(CN)₂ and Cd(CN)₂ structures and the synthesis and structure of the diamond-related frameworks [N(CH₃)₄][Cu₂Zn^{II}(CN)₄] and Cu^I[4,4’,4’’-tetracyanotetraphenylmethane]BF₄·x C₆H₅NO₂. *J. Am. Chem. Soc.* **112**, 1546–1554 (1990).
9. O. M. Yaghi, H. Li, Hydrothermal synthesis of a metal–organic framework containing large rectangular channels. *J. Am. Chem. Soc.* **117**, 10401–10402 (1995).
10. S. Subramanian, M. J. Zaworotko, Porous solids by design: [Zn(4,4’-bpy)₂(SiF₆)₂]_n·xDMF, a single framework octahedral coordination polymer with large square channels. *Angew. Chem. Int. Ed. Engl.* **34**, 2127–2129 (1995).
11. H. Li, M. Eddaoudi, T. L. Groy, O. M. Yaghi, Establishing microporosity in open metal–organic frameworks: Gas sorption isotherms for Zn(BDC) (BDC = 1,4-benzenedicarboxylate). *J. Am. Chem. Soc.* **120**, 8571–8572 (1998).
12. J. Jiang, Y. Zhao, O. M. Yaghi, Covalent chemistry beyond molecules. *J. Am. Chem. Soc.* **138**, 3255–3265 (2016).
13. M. Kondo, T. Yoshitomi, H. Matsuzaka, S. Kitagawa, K. Seki, Three-dimensional framework with channeling cavities for small molecules: {[M₂(4, 4’-bpy)₃(NO₃)₄·xH₂O]_n} (M = Co, Ni, Zn). *Angew. Chem. Int. Ed. Engl.* **36**, 1725–1727 (1997).
14. H. Li, M. Eddaoudi, M. O’Keeffe, O. M. Yaghi, Design and synthesis of an exceptionally stable and highly porous metal–organic framework. *Nature* **402**, 276–279 (1999).
15. S. S.-Y. Chui, S. M.-F. Lo, J. P. Charmant, A. G. Orpen, I. D. Williams, A chemically functionalizable nanoporous material [Cu₃(TMA)₂(H₂O)₃]_n. *Science* **283**, 1148–1150 (1999).
16. F. Gándara, H. Furukawa, S. Lee, O. M. Yaghi, High methane storage capacity in aluminum metal–organic frameworks. *J. Am. Chem. Soc.* **136**, 5271–5274 (2014).
17. K. Sumida, M. R. Hill, S. Horike, A. Dailly, J. R. Long, Synthesis and hydrogen storage properties of Be₁₂(OH)₁₂(1,3,5-benzenetribenzoate)₄. *J. Am. Chem. Soc.* **131**, 15120–15121 (2009).
18. A. Schoedel, M. Li, D. Li, M. O’Keeffe, O. M. Yaghi, Structures of metal–organic frameworks with rod secondary building units. *Chem. Rev.* **116**, 12466–12535 (2016).
19. H. Furukawa, N. Ko, Y. B. Go, N. Aratani, S. B. Choi, E. Choi, A. Ö. Yazaydin, R. Q. Snurr, M. O’Keeffe, J. Kim, O. M. Yaghi, Ultrahigh porosity in metal–organic frameworks. *Science* **329**, 424–428 (2010).
20. O. K. Farha, I. Eryazici, N. C. Jeong, B. G. Hauser, C. E. Wilmer, A. A. Sarjeant, R. Q. Snurr, S. T. Nguyen, A. Ö. Yazaydin, J. T. Hupp, Metal–organic framework materials with ultrahigh surface areas: Is the sky the limit? *J. Am. Chem. Soc.* **134**, 15016–15021 (2012).
21. M. Li, D. Li, M. O’Keeffe, O. M. Yaghi, Topological analysis of metal–organic frameworks with polytopic linkers and/or multiple building units and the minimal transitivity principle. *Chem. Rev.* **114**, 1343–1370 (2014).
22. M. Eddaoudi, D. B. Moler, H. Li, B. Chen, T. M. Reineke, M. O’Keeffe, O. M. Yaghi, Modular chemistry: Secondary building units as a basis for the design of highly porous and robust metal–organic carboxylate frameworks. *Acc. Chem. Res.* **34**, 319–330 (2001).
23. M. Eddaoudi, J. Kim, N. Rosi, D. Vodak, J. Wachter, M. O’Keeffe, O. M. Yaghi, Systematic design of pore size and functionality in isoreticular MOFs and their application in methane storage. *Science* **295**, 469–472 (2002).
24. G. Férey, C. Serre, C. Mellot-Draznieks, F. Millange, S. Surlblé, J. Dutour, I. Margiolaki, A hybrid solid with giant pores prepared by a combination of targeted chemistry, simulation, and powder diffraction. *Angew. Chem. Int. Ed. Engl.* **43**, 6296–6301 (2004).
25. D. Feng, T.-F. Liu, J. Su, M. Bosch, Z. Wei, W. Wan, D. Yuan, Y.-P. Chen, X. Wang, K. Wang, X. Lian, Z.-Y. Gu, J. Park, X. Zou, H.-C. Zhou, Stable metal–organic frameworks containing single-molecule traps for enzyme encapsulation. *Nat. Commun.* **6**, 5979 (2015).
26. H. Deng, S. Grunler, K. E. Cordova, C. Valente, H. Furukawa, M. Hmadeh, F. Gándara, A. C. Whalley, Z. Liu, S. Asahina, H. Kazumori, M. O’Keeffe, O. Terasaki, J. F. Stoddart, O. M. Yaghi, Large-pore apertures in a series of metal–organic frameworks. *Science* **336**, 1018–1023 (2012).
27. W. Morris, B. Voloskiy, S. Demir, F. Gándara, P. L. McGrier, H. Furukawa, D. Cascio, J. F. Stoddart, O. M. Yaghi, Synthesis, structure, and metalation of two new highly porous zirconium metal–organic frameworks. *Inorg. Chem.* **51**, 6443–6445 (2012).
28. P. Deria, D. A. Gómez-Gualdrón, I. Hod, R. Q. Snurr, J. T. Hupp, O. K. Farha, Framework-topology-dependent catalytic activity of zirconium-based (porphyrinato)zinc(II) MOFs. *J. Am. Chem. Soc.* **138**, 14449–14457 (2016).
29. H.-L. Jiang, D. Feng, K. Wang, Z.-Y. Gu, Z. Wei, Y.-P. Chen, H.-C. Zhou, An exceptionally stable, porphyrinic Zr metal–organic framework exhibiting pH-dependent fluorescence. *J. Am. Chem. Soc.* **135**, 13934–13938 (2013).
30. Q. Liu, H. Cong, H. Deng, Deciphering the spatial arrangement of metals and correlation to reactivity in multivariate metal–organic frameworks. *J. Am. Chem. Soc.* **138**, 13822–13825 (2016).
31. D. J. Tranchemontagne, K. S. Park, H. Furukawa, J. Eckert, C. B. Knobler, O. M. Yaghi, Hydrogen storage in new metal–organic frameworks. *J. Phys. Chem. C* **116**, 13143–13151 (2012).
32. B. Tu, Q. Pang, H. Xu, X. Li, Y. Wang, Z. Ma, L. Weng, Q. Li, Reversible redox activity in multicomponent metal–organic frameworks constructed from trinuclear copper pyrazolate building blocks. *J. Am. Chem. Soc.* **139**, 7998–8007 (2017).
33. B. Tu, Q. Pang, E. Ning, W. Yan, Y. Qi, D. Wu, Q. Li, Heterogeneity within a mesoporous metal–organic framework with three distinct metal-containing building units. *J. Am. Chem. Soc.* **137**, 13456–13459 (2015).
34. M. Eddaoudi, J. Kim, J. B. Wachter, H. K. Chae, M. O’Keeffe, O. M. Yaghi, Porous metal–organic polyhedra: 25 A cuboctahedron constructed from 12 Cu₂(CO₃)₄ paddle-wheel building blocks. *J. Am. Chem. Soc.* **123**, 4368–4369 (2001).
35. F. Nouar, J. F. Eubank, T. Bousquet, L. Wojtas, M. J. Zaworotko, M. Eddaoudi, Supermolecular building blocks (SBBs) for the design and synthesis of highly porous metal–organic frameworks. *J. Am. Chem. Soc.* **130**, 1833–1835 (2008).
36. J. F. Eubank, F. Nouar, R. Luebke, A. J. Cairns, L. Wojtas, M. Alkordi, T. Bousquet, M. R. Hight, J. Eckert, J. P. Embs, P. A. Georgiev, M. Eddaoudi, On demand: The singular rht net, an ideal blueprint for the construction of a metal–organic framework (MOF) platform. *Angew. Chem. Int. Ed. Engl.* **51**, 10099–10103 (2012).
37. T. Pham, K. A. Forrest, A. Hogan, K. McLaughlin, J. L. Belof, J. Eckert, B. Space, Simulations of hydrogen sorption in rht-MOF-1: Identifying the binding sites through explicit polarization and quantum rotation calculations. *J. Mater. Chem. A* **2**, 2088–2100 (2014).
38. A. J. Cairns, J. A. Perman, L. Wojtas, V. Ch. Kravtsov, M. H. Alkordi, M. Eddaoudi, M. J. Zaworotko, Supermolecular building blocks (SBBs) and crystal design: 12-connected open frameworks based on a molecular cubohemioctahedron. *J. Am. Chem. Soc.* **130**, 1560–1561 (2008).
39. V. Guillerme, D. Kim, J. F. Eubank, R. Luebke, X. Liu, K. Adil, M. S. Lah, M. Eddaoudi, A supermolecular building approach for the design and construction of metal–organic frameworks. *Chem. Soc. Rev.* **43**, 6141–6172 (2014).
40. S. Yuan, J.-S. Qin, J. Li, L. Huang, L. Feng, Y. Fang, C. Lollar, J. Pang, L. Zhang, D. Sun, A. Alsalmé, T. Cagin, H.-C. Zhou, Retrosynthesis of multi-component metal–organic frameworks. *Nat. Commun.* **9**, 808 (2018).
41. H. Li, C. E. Davis, T. L. Groy, D. G. Kelley, O. M. Yaghi, Coordinatively unsaturated metal centers in the extended porous framework of Zn₃(BDC)₃·6CH₃OH (BDC = 1,4-benzenedicarboxylate). *J. Am. Chem. Soc.* **120**, 2186–2187 (1998).
42. B. Chen, M. Eddaoudi, T. M. Reineke, J. W. Kampf, M. O’Keeffe, O. M. Yaghi, Cu₂(ATC)·6H₂O: Design of open metal sites in porous metal–organic crystals (ATC: 1,3,5,7-adamantane tetracarboxylate). *J. Am. Chem. Soc.* **122**, 11559–11560 (2000).
43. Y. He, B. Chen, in *Encyclopedia of Inorganic and Bioinorganic Chemistry* (John Wiley & Sons Ltd., 2011).
44. Y. K. Hwang, D.-Y. Hong, J.-S. Chang, S. H. Jhung, Y.-K. Seo, J. Kim, A. Vimont, M. Daturi, C. Serre, G. Férey, Amine grafting on coordinatively unsaturated metal centers of MOFs: Consequences for catalysis and metal encapsulation. *Angew. Chem. Int. Ed. Engl.* **47**, 4144–4148 (2008).
45. T. M. McDonald, D. M. D’Alessandro, R. Krishna, J. R. Long, Enhanced carbon dioxide capture upon incorporation of N,N’-dimethylethylenediamine in the metal–organic framework CuBTTri. *Chem. Sci.* **2**, 2022–2028 (2011).
46. P. J. Milner, R. L. Siegelman, A. C. Forse, M. I. Gonzalez, T. Runčevski, J. D. Martell, J. A. Reimer, J. R. Long, A diaminopropane-appended metal–organic framework enabling efficient CO₂ capture from coal flue gas via a mixed adsorption mechanism. *J. Am. Chem. Soc.* **139**, 13541–13553 (2017).
47. S. Lee, E. A. Kapustin, O. M. Yaghi, Coordinative alignment of molecules in chiral metal–organic frameworks. *Science* **353**, 808–811 (2016).
48. J. Jiang, F. Gándara, Y.-B. Zhang, K. Na, O. M. Yaghi, W. G. Klemperer, Superacidity in sulfated metal–organic framework-808. *J. Am. Chem. Soc.* **136**, 12844–12847 (2014).
49. S. Yuan, W. Lu, Y.-P. Chen, Q. Zhang, T.-F. Liu, D. Feng, X. Wang, J. Qin, H.-C. Zhou, Sequential linker installation: Precise placement of functional groups in multivariate metal–organic frameworks. *J. Am. Chem. Soc.* **137**, 3177–3180 (2015).

50. E. A. Kapustin, S. Lee, A. S. Alshammari, O. M. Yaghi, Molecular retrofitting adapts a metal–organic framework to extreme pressure. *ACS Cent. Sci.* **3**, 662–667 (2017).
51. B. Tu, Q. Pang, D. Wu, Y. Song, L. Weng, Q. Li, Ordered vacancies and their chemistry in metal–organic frameworks. *J. Am. Chem. Soc.* **136**, 14465–14471 (2014).
52. M. Kim, J. F. Cahill, Y. Su, K. A. Prather, S. M. Cohen, Postsynthetic ligand exchange as a route to functionalization of ‘inert’ metal–organic frameworks. *Chem. Sci.* **3**, 126–130 (2012).
53. J. An, O. K. Farha, J. T. Hupp, E. Pohl, J. I. Yeh, N. L. Rosi, Metal-adeninate vertices for the construction of an exceptionally porous metal-organic framework. *Nat. Commun.* **3**, 604 (2012).
54. T. Li, M. T. Kozłowski, E. A. Doud, M. N. Blakely, N. L. Rosi, Stepwise ligand exchange for the preparation of a family of mesoporous MOFs. *J. Am. Chem. Soc.* **135**, 11688–11691 (2013).
55. C. K. Brozek, M. Dincă, Cation exchange at the secondary building units of metal–organic frameworks. *Chem. Soc. Rev.* **43**, 5456–5467 (2014).
56. H. Irving, R. J. P. Williams, The stability of transition-metal complexes. *J. Chem. Soc. (Resumed)* **0**, 3192–3210 (1953).
57. M. Kim, J. F. Cahill, H. Fei, K. A. Prather, S. M. Cohen, Postsynthetic ligand and cation exchange in robust metal–organic frameworks. *J. Am. Chem. Soc.* **134**, 18082–18088 (2012).
58. M. S. Denny Jr., L. R. Parent, J. P. Patterson, S. K. Meena, H. Pham, P. Abellan, Q. M. Ramasse, F. Paesani, N. C. Gianneschi, S. M. Cohen, Transmission electron microscopy reveals deposition of metal oxide coatings onto metal–organic frameworks. *J. Am. Chem. Soc.* **140**, 1348–1357 (2018).
59. C. K. Brozek, M. Dincă, Ti^{3+} , $V^{2+/3+}$, $Cr^{2+/3+}$, Mn^{2+} , and Fe^{2+} -substituted MOF-5 and redox reactivity in Cr- and Fe-MOF-5. *J. Am. Chem. Soc.* **135**, 12886–12891 (2013).
60. T.-F. Liu, L. Zou, D. Feng, Y.-P. Chen, S. Fordham, X. Wang, Y. Liu, H.-C. Zhou, Stepwise synthesis of robust metal–organic frameworks via postsynthetic metathesis and oxidation of metal nodes in a single-crystal to single-crystal transformation. *J. Am. Chem. Soc.* **136**, 7813–7816 (2014).
61. N. Planas, J. E. Mondloch, S. Tussupbayev, J. Borycz, L. Gagliardi, J. T. Hupp, O. K. Farha, C. J. Cramer, Defining the proton topology of the Zr_6 -based metal–organic framework NU-1000. *J. Phys. Chem. Lett.* **5**, 3716–3723 (2014).
62. M. Meilikhov, K. Yusenko, R. A. Fischer, Turning MIL-53(Al) redox-active by functionalization of the bridging OH-group with 1,1'-ferrocenediyl-dimethylsilane. *J. Am. Chem. Soc.* **131**, 9644–9645 (2009).
63. H. Li, K. Wang, Y. Sun, C. T. Lollar, J. Li, H.-C. Zhou, Recent advances in gas storage and separation using metal–organic frameworks. *Mater. Today* **21**, 108–121 (2018).
64. A. H. Chughtai, N. Ahmad, H. A. Younus, A. Laypkov, F. Verpoort, Metal–organic frameworks: Versatile heterogeneous catalysts for efficient catalytic organic transformations. *Chem. Soc. Rev.* **44**, 6804–6849 (2015).
65. Y. Zhang, S. Yuan, G. Day, X. Wang, X. Yang, H.-C. Zhou, Luminescent sensors based on metal–organic frameworks. *Coord. Chem. Rev.* **354**, 28–45 (2018).
66. M.-X. Wu, Y.-W. Yang, Metal–organic framework (MOF)-based drug/cargo delivery and cancer therapy. *Adv. Mater.* **29**, 1606134 (2017).
67. J. L. C. Rowsell, E. C. Spencer, J. Eckert, J. A. K. Howard, O. M. Yaghi, Gas adsorption sites in a large-pore metal-organic framework. *Science* **309**, 1350–1354 (2005).
68. J. L. C. Rowsell, J. Eckert, O. M. Yaghi, Characterization of H_2 binding sites in prototypical metal–organic frameworks by inelastic neutron scattering. *J. Am. Chem. Soc.* **127**, 14904–14910 (2005).
69. J. A. Greathouse, T. L. Kinniburgh, M. D. Allendorf, Adsorption and separation of noble gases by IRMOF-1: Grand canonical Monte Carlo simulations. *Ind. Eng. Chem. Res.* **48**, 3425–3431 (2009).
70. M. Dincă, J. R. Long, Hydrogen storage in microporous metal–organic frameworks with exposed metal sites. *Angew. Chem. Int. Ed. Engl.* **47**, 6766–6779 (2008).
71. A. D. Wiersum, J.-S. Chang, C. Serre, P. L. Llewellyn, An adsorbent performance indicator as a first step evaluation of novel sorbents for gas separations: Application to metal-organic frameworks. *Langmuir* **29**, 3301–3309 (2013).
72. P. D. C. Dietzel, R. E. Johnsen, H. Fjellvåg, S. Bordiga, E. Groppo, S. Chavan, R. Blom, Adsorption properties and structure of CO_2 adsorbed on open coordination sites of metal–organic framework $Ni_2(dhtp)$ from gas adsorption, IR spectroscopy and X-ray diffraction. *Chem. Commun.* **0**, 5125–5127 (2008).
73. A. K. Kizzie, A. G. Wong-Foy, A. J. Matzger, Effect of humidity on the performance of microporous coordination polymers as adsorbents for CO_2 capture. *Langmuir* **27**, 6368–6373 (2011).
74. G. T. Rochelle, Amine scrubbing for CO_2 capture. *Science* **325**, 1652–1654 (2009).
75. T. M. McDonald, J. A. Mason, X. Kong, E. D. Bloch, D. Gygi, A. Dani, V. Crocellà, F. Giordanino, S. O. Odoh, W. S. Drisdell, B. Vlasisavljević, A. L. Dzubak, R. Poloni, S. K. Schnell, N. Planas, K. Lee, T. Pascal, L. F. Wan, D. Prendergast, J. B. Neaton, B. Smit, J. B. Kortright, L. Gagliardi, S. Bordiga, J. A. Reimer, J. R. Long, Cooperative insertion of CO_2 in diamine-appended metal-organic frameworks. *Nature* **519**, 303–308 (2015).
76. T. M. McDonald, W. R. Lee, J. A. Mason, B. M. Wiers, C. S. Hong, J. R. Long, Capture of carbon dioxide from air and flue gas in the alkylamine-appended metal–organic framework mmen- $Mg_2(dobpdc)$. *J. Am. Chem. Soc.* **134**, 7056–7065 (2012).
77. P.-Q. Liao, H. Chen, D.-D. Zhou, S.-Y. Liu, C.-T. He, Z. Rui, H. Ji, J.-P. Zhang, X.-M. Chen, Monodentate hydroxide as a super strong yet reversible active site for CO_2 capture from high-humidity flue gas. *Energ. Environ. Sci.* **8**, 1011–1016 (2015).
78. Z. Bao, G. Chang, H. Xing, R. Krishna, Q. Ren, B. Chen, Potential of microporous metal–organic frameworks for separation of hydrocarbon mixtures. *Energ. Environ. Sci.* **9**, 3612–3641 (2016).
79. E. D. Bloch, W. L. Queen, R. Krishna, J. M. Zadrozny, C. M. Brown, J. R. Long, Hydrocarbon separations in a metal-organic framework with open iron(ii) coordination sites. *Science* **335**, 1606–1610 (2012).
80. S. J. Geier, J. A. Mason, E. D. Bloch, W. L. Queen, M. R. Hudson, C. M. Brown, J. R. Long, Selective adsorption of ethylene over ethane and propylene over propane in the metal–organic frameworks $M_2(dobdc)$ ($M = Mg, Mn, Fe, Co, Ni, Zn$). *Chem. Sci.* **4**, 2054–2061 (2013).
81. S. Mukherjee, B. Manna, A. V. Desai, Y. Yin, R. Krishna, R. Babarao, S. K. Ghosh, Harnessing Lewis acidic open metal sites of metal–organic frameworks: The foremost route to achieve highly selective benzene sorption over cyclohexane. *Chem. Commun.* **52**, 8215–8218 (2016).
82. S. Yang, A. J. Ramirez-Cuesta, R. Newby, V. Garcia-Sakai, P. Manuel, S. K. Callear, S. I. Campbell, C. C. Tang, M. Schröder, Supramolecular binding and separation of hydrocarbons within a functionalized porous metal–organic framework. *Nat. Chem.* **7**, 121–129 (2015).
83. A. J. Rieth, S. Yang, E. N. Wang, M. Dincă, Record atmospheric fresh water capture and heat transfer with a material operating at the water uptake reversibility limit. *ACS Cent. Sci.* **3**, 668–672 (2017).
84. S. M. Towsif Abtab, D. Alezi, P. M. Bhatt, A. Shkurenko, Y. Belmabkhout, H. Aggarwal, Ł. J. Weseliński, N. Alsdun, U. Samin, M. N. Hedhili, M. Eddaoudi, Reticular chemistry in action: A hydrolytically stable MOF capturing twice its weight in adsorbed water. *Chem.* **4**, 94–105 (2018).
85. F. Fathieh, M. J. Kalmutzki, E. A. Kapustin, P. J. Waller, J. Yang, O. M. Yaghi, Practical water production from desert air. *Sci. Adv.* **4**, eaat3198 (2018).
86. M. J. Kalmutzki, C. S. Diercks, O. M. Yaghi, Metal–organic frameworks for water harvesting from air. *Adv. Mater.*, 1704304 (2018).
87. H. Furukawa, F. Gándara, Y.-B. Zhang, J. Jiang, W. L. Queen, M. R. Hudson, O. M. Yaghi, Water adsorption in porous metal–organic frameworks and related materials. *J. Am. Chem. Soc.* **136**, 4369–4381 (2014).
88. D. D. Borges, G. Maurin, D. S. Galvão, Design of porous metal-organic frameworks for adsorption driven thermal batteries. *MRS Adv.* **2**, 519–524 (2017).
89. C. S. Diercks, Y. Liu, K. E. Cordova, O. M. Yaghi, The role of reticular chemistry in the design of CO_2 reduction catalysts. *Nat. Mater.* **17**, 301–307 (2018).
90. J. E. Mondloch, O. K. Farha, J. T. Hupp, Catalysis at the organic ligands, in *Metal Organic Frameworks as Heterogeneous Catalysts*, F. X. Llabrés i Xamena, J. Gascon, Eds. (Royal Society of Chemistry, 2013), pp. 289–309.
91. F. Vermoortele, P. Valckens, D. De Vos, Catalysis at the metallic nodes of MOFs, in *Metal Organic Frameworks as Heterogeneous Catalysts*, F. X. Llabrés i Xamena, J. Gascon, Eds. (The Royal Society of Chemistry, 2013), pp. 268–288.
92. K. Schlichte, T. Kratzke, S. Kaskel, Improved synthesis, thermal stability and catalytic properties of the metal-organic framework compound $CU_3(BTC)_2$. *Microporous Mesoporous Mater.* **73**, 81–88 (2004).
93. A. Henschel, K. Gedrich, R. Kraehnert, S. Kaskel, Catalytic properties of MIL-101. *Chem. Commun.* **21**, 4192–4194 (2008).
94. R. J. Comito, K. J. Fritzsche, B. J. Sundell, K. Schmidt-Rohr, M. Dincă, Single-site heterogeneous catalysts for olefin polymerization enabled by cation exchange in a metal-organic framework. *J. Am. Chem. Soc.* **138**, 10232–10237 (2016).
95. E. D. Metzger, C. K. Brozek, R. J. Comito, M. Dincă, Selective dimerization of ethylene to 1-butene with a porous catalyst. *ACS Cent. Sci.* **2**, 148–153 (2016).
96. D. Denysenko, T. Werner, M. Grzywa, A. Puls, V. Hagen, G. Eicklerling, J. Jelic, K. Reuter, D. Volkmer, Reversible gas-phase redox processes catalyzed by Co-exchanged MFU-4l(arge). *Chem. Commun.* **48**, 1236–1238 (2012).
97. E. D. Metzger, R. J. Comito, C. H. Hendon, M. Dincă, Mechanism of single-site molecule-like catalytic ethylene dimerization in Ni-MFU-4l. *J. Am. Chem. Soc.* **139**, 757–762 (2017).
98. I. S. Kim, J. Borycz, A. E. Platero-Prats, S. Tussupbayev, T. C. Wang, O. K. Farha, J. T. Hupp, L. Gagliardi, K. W. Chapman, C. J. Cramer, A. B. F. Martinson, Targeted single-site MOF node modification: Trivalent metal loading via atomic layer deposition. *Chem. Mater.* **27**, 4772–4778 (2015).
99. K. Manna, P. Ji, Z. Lin, F. X. Greene, A. Urban, N. C. Thacker, W. Lin, Chemosselective single-site Earth-abundant metal catalysts at metal-organic framework nodes. *Nat. Commun.* **7**, 12610 (2016).
100. J. E. Mondloch, W. Bury, D. Fairen-Jimenez, S. Kwon, E. J. DeMarco, M. H. Weston, A. A. Sarjeant, S. T. Nguyen, P. C. Stair, R. Q. Snurr, O. K. Farha, J. T. Hupp, Vapor-phase

- metalation by atomic layer deposition in a metal-organic framework. *J. Am. Chem. Soc.* **135**, 10294–10297 (2013).
101. T. Ikuno, J. Zheng, A. Vjunov, M. Sanchez-Sanchez, M. A. Ortuño, D. R. Pahls, J. L. Fulton, D. M. Camaioni, Z. Li, D. Ray, B. L. Mehdi, N. D. Browning, O. K. Farha, J. T. Hupp, C. J. Cramer, L. Gagliardi, J. A. Lercher, Methane oxidation to methanol catalyzed by Cu-Oxo clusters stabilized in NU-1000 metal-organic framework. *J. Am. Chem. Soc.* **139**, 10294–10301 (2017).
102. J. Jiang, O. M. Yaghi, Brønsted acidity in metal-organic frameworks. *Chem. Rev.* **115**, 6966–6997 (2015).
103. M. Dan-Hardi, C. Serre, T. Frot, L. Rozes, G. Maurin, C. Sanchez, G. Férey, A new photoactive crystalline highly porous titanium(IV) dicarboxylate. *J. Am. Chem. Soc.* **131**, 10857–10859 (2009).
104. M. W. Logan, S. Ayad, J. D. Adamson, T. Dilbeck, K. Hanson, F. J. Uribe-Romo, Systematic variation of the optical bandgap in titanium based isorecticular metal-organic frameworks for photocatalytic reduction of CO₂ under blue light. *J. Mater. Chem. A* **5**, 11854–11863 (2017).
105. Y. Fu, D. Sun, Y. Chen, R. Huang, Z. Ding, X. Fu, Z. Li, An amine-functionalized titanium metal-organic framework photocatalyst with visible-light-induced activity for CO₂ reduction. *Angew. Chem. Int. Ed. Engl.* **51**, 3364–3367 (2012).
106. H. L. Nguyen, The chemistry of titanium-based metal-organic frameworks. *New J. Chem.* **41**, 14030–14043 (2017).
107. H. L. Nguyen, F. Gándara, H. Furukawa, T. L. H. Doan, K. E. Cordova, O. M. Yaghi, A titanium-organic framework as an exemplar of combining the chemistry of metal- and covalent-organic frameworks. *J. Am. Chem. Soc.* **138**, 4330–4333 (2016).
108. P. J. Waller, F. Gándara, O. M. Yaghi, Chemistry of covalent organic frameworks. *Acc. Chem. Res.* **48**, 3053–3063 (2015).
109. S. Yuan, J. S. Qin, H. Q. Xu, J. Su, D. Rossi, Y. Chen, L. Zhang, C. Lollar, Q. Wang, H. L. Jiang, D. H. Son, H. Xu, Z. Huang, X. Zou, H. C. Zhou, [Ti₆Zr₂O₁₂(COO)₁₆] cluster: An ideal inorganic building unit for photoactive metal-organic frameworks. *ACS Cent. Sci.* **4**, 105–111 (2018).
110. M. O'Keeffe, M. A. Peskov, S. J. Ramsden, O. M. Yaghi, The Reticular Chemistry Structure Resource (RCSR) database of, and symbols for, crystal nets. *Acc. Chem. Res.* **41**, 1782–1789 (2008).

Acknowledgments: O.M.Y. acknowledges the contributions of the many graduate students and postdoctoral fellows whose work is being summarized and cited in this review and is being recognized by the BBVA Frontiers of Knowledge Award in the Basic Sciences 2018.

Funding: This work was supported by the funding from the Badische Anilin- & Soda-Fabrik (BASF) SE and King Abdulaziz City for Science and Technology. M.J.K. is grateful for financial support through the German Research Foundation (DFG, KA 4484/1-1). **Author contributions:** All authors conceived the ideas and planned the content. M.J.K. and N.H. wrote the first draft. All authors worked on the final draft. **Competing interests:** The authors declare that they have no competing financial, professional, or personal interests that might have influenced the performance or presentation of the work described in this manuscript. **Data and materials availability:** All data needed to evaluate the conclusions in the paper are present in the paper and/or the materials cited herein. Additional data related to this paper may be requested from the authors.

Submitted 18 April 2018

Accepted 28 August 2018

Published 5 October 2018

10.1126/sciadv.aat9180

Citation: M. J. Kalmutzki, N. Hanikel, O. M. Yaghi, Secondary building units as the turning point in the development of the reticular chemistry of MOFs. *Sci. Adv.* **4**, eaat9180 (2018).